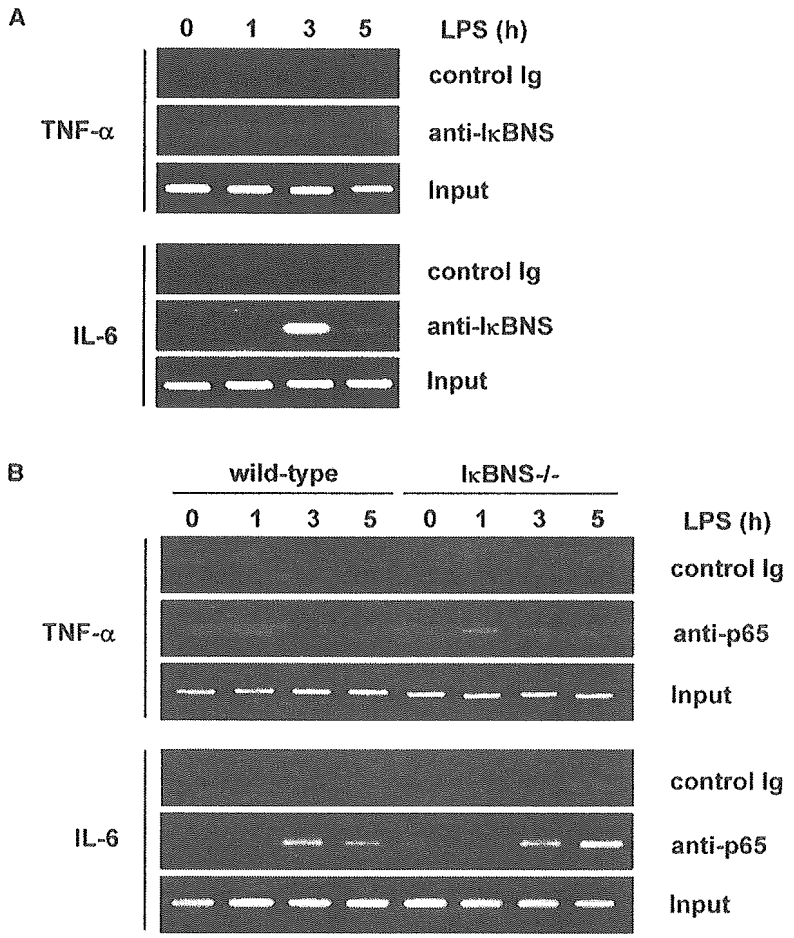

Figure 5. IκBNS Regulation of p65 Activity at the IL-6 Promoter

(A) Wild-type bone marrow-derived macrophages were stimulated with 100 ng/ml of LPS for the indicated periods, and chromatin immunoprecipitation (ChIP) assay was performed with anti-IκBNS Ab or control Ig. The immunoprecipitated TNF-α promoter (upper panel) or IL-6 promoter (lower panel) was analyzed by PCR with promoter-specific primers. PCR amplification of the total input DNA in each sample is shown (Input). Representative of three independent experiments. The same result was obtained when peritoneal macrophages were used.

(B) Macrophages from wild-type or IκBNS$^{-/-}$ mice were stimulated with LPS for the indicated periods. Then, ChIP assay was performed with anti-p65 Ab or control Ig. The immunoprecipitated TNF-α promoter (upper panel) or IL-6 promoter (lower panel) was analyzed by PCR with promoter-specific primers. Representative of three independent experiments.

the IL-6 promoter, but not at the TNF-α promoter, was prolonged in LPS-stimulated IκBNS$^{-/-}$ macrophages. Taken together, these findings indicate that TLR-inducible IκBNS is responsible for termination of NF-κB activity through its recruitment to specific promoters.

High Sensitivity to LPS-Induced Endotoxin Shock in IκBNS-Deficient Mice

To study the in vivo role of IκBNS, we examined LPS-induced endotoxin shock. Intraperitoneal injection of LPS resulted in marked increases in serum concentrations of TNF-α, IL-6, and IL-12p40 (Figure 6A). TNF-α level was comparable between wild-type and IκBNS$^{-/-}$ mice, which rapidly peaked at around 1.5 hr of LPS administration. In the case of IL-6 and IL-12p40 levels, concentrations of both cytokines were almost equally elevated within 3 hr of LPS injection. After 3 hr, levels of both cytokines gradually decreased in wild-type mice. However, concentrations of IL-6 and IL-12p40 sustained, rather enhanced, in IκBNS$^{-/-}$ mice after 3 hr. Thus, persistently high concentrations of LPS-induced serum IL-6 and IL-12p40 were observed in IκBNS$^{-/-}$ mice. Furthermore, high sensitivity to LPS-induced lethality was observed in IκBNS$^{-/-}$ mice (Figure 6B). All IκBNS$^{-/-}$ mice died within 4 days of LPS challenge at a dose of which almost all wild-type mice survived over 4 days. These findings indicate that IκBNS$^{-/-}$ mice are highly sensitive to LPS-induced endotoxin shock.

High Susceptibility to DSS-Induced Colitis in IκBNS$^{-/-}$ Mice

In a previous report, IκBNS was shown to be constitutively expressed in macrophages residing in the colonic lamina propria, which explains one of the mechanisms for hyporesponsiveness to TLR stimulation in these cells (Hirotani et al., 2005). Therefore, we next stimulated CD11b^{+} cells isolated from the colonic lamina propria with LPS and analyzed for production of TNF-α and IL-6 (Figure S4). In CD11b^{+} cells from wild-type mice, LPS-induced production of these cytokines was not significantly observed. In cells from IκBNS$^{-/-}$ mice, IL-6 production was increased even in the absence of stimulation, and LPS stimulation led to markedly enhanced production of IL-6, but not TNF-α. In the next experiment, in order to expose these cells to microflora and cause intestinal inflammation, mice were orally administered with dextran sodium sulfate (DSS), which is toxic to colonic epithelial cells and therefore disrupts the epithelial cell barrier (Kitajima et al., 1999). IκBNS$^{-/-}$ mice showed more severe weight loss compared with wild-type mice (Figure 7A). Histological analyses of the colon indicated that the inflammatory lesions were more severe and more extensive in IκBNS$^{-/-}$ mice (Figures 7B and 7C). Thus, IκBNS$^{-/-}$ mice are highly susceptible to intestinal inflammation. Th1-oriented CD4^{+} T cell response was shown to be associated with DSS colitis (Strober et al., 2002). Therefore, we analyzed IFN-γ

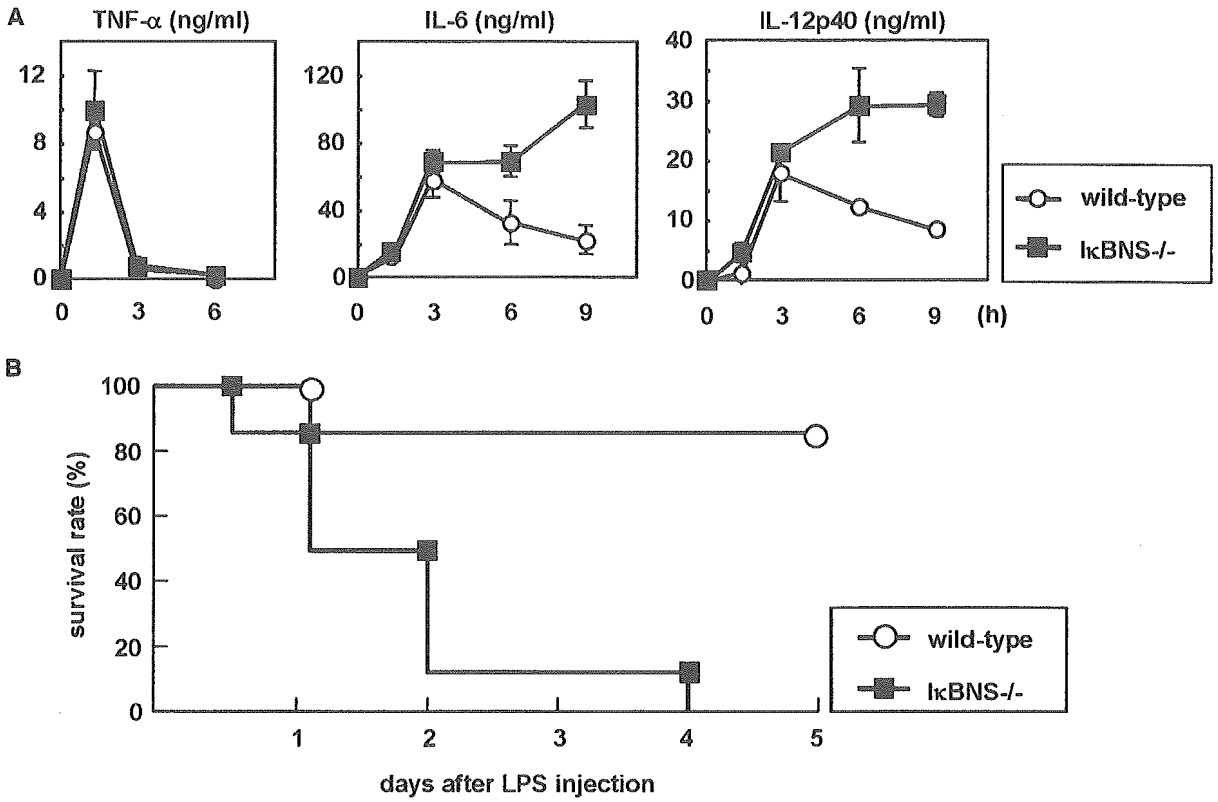

Figure 6. High Susceptibility to LPS-Induced Endotoxin Shock in IκBNS$^{-/-}$ Mice

Age-matched wild-type (n = 6) and IκBNS−/− (n = 6) mice were intraperitoneally injected with LPS (1 mg). (A) Sera were taken at 1.5, 3, 6, and 9 hr after LPS injection. Serum concentrations of TNF-α, IL-6, and IL-12p40 were determined by ELISA. Results are shown as mean ± SD of serum samples from six mice. (B) Survival was monitored for 5 days.

production from splenic CD4$^+$ T cells of wild-type and IκBNS$^{-/-}$ mice before and after DSS administration (Figure 7D). DSS administration led to a mild increase in IFN-γ production in wild-type mice. In nontreated IκBNS$^{-/-}$ mice, IFN-γ production was slightly increased compared with nontreated wild-type mice. In DSS-fed IκBNS$^{-/-}$ mice, a significant increase in IFN-γ production was observed compared to DSS-fed wild-type mice. These results indicate that IκBNS$^{-/-}$ mice are susceptible to intestinal inflammation caused by exposure to microflora.

Discussion

In the present study, we characterized the physiological function of IκBNS. Induced by TLR stimulation, IκBNS is involved in termination of NF-κB activity and thereby inhibits a subset of TLR-dependent genes that are induced late through MyD88-dependent NF-κB activation. Accordingly, IκBNS$^{-/-}$ mice show sustained production of IL-6 and IL-12p40, resulting in high susceptibility to LPS-induced endotoxin shock. Furthermore, IκBNS$^{-/-}$ mice are susceptible to intestinal inflammation accompanied by enhanced Th1 responses.

IκBNS was originally identified as a molecule that mediates negative selection of thymocytes (Fiorini et al., 2002). However, IκBNS$^{-/-}$ mice did not show any defect in T cell development. Requirement of IκBNS in negative selection of thymocytes should be analyzed precisely using peptide-specific TCR transgenic mice, such as mice bearing the H-Y TCR, in the future (Kisielow et al., 1988).

Recent studies have established that TLR-dependent gene induction is regulated mainly by NF-κB and IRF families of transcription factors (Akira and Takeda, 2004; Honda et al., 2005; Takaoka et al., 2005). In TLR4 signaling, the TRIF-dependent pathway is responsible for induction of IFN-β and IFN-inducible genes through activation of IRF-3, whereas the MyD88-dependent pathway mediates induction of several NF-κB dependent genes (Beutler, 2004). A study with mice lacking IκBζ, another member of nuclear IκB proteins, has demonstrated that the MyD88-dependent genes are divided into at least two types; one is induced early and independent of IκBζ, and another is induced late and dependent on IκBζ (Yamamoto et al., 2004). The IκBζ-regulated genes include IL-6, IL-12p40, IL-18, and G-CSF, which are all upregulated in LPS-stimulated IκBNS$^{-/-}$ macrophages. Thus, IκBNS seems to possess a function quite opposite to IκBζ. IκBNS is most structurally related to IκBζ (Fiorini et al., 2002; Hirotani et al., 2005). But, IκBζ has an additional N-terminal structure, which seemingly mediates the induction of target genes (Motoyama et al., 2005). Thus, nuclear IκB proteins IκBζ and IκBNS positively and negatively regulate a subset of TLR-induced NF-κB-dependent genes, respectively.

Recently, negative regulation of TLR-dependent gene induction was extensively analyzed (Liew et al., 2005).

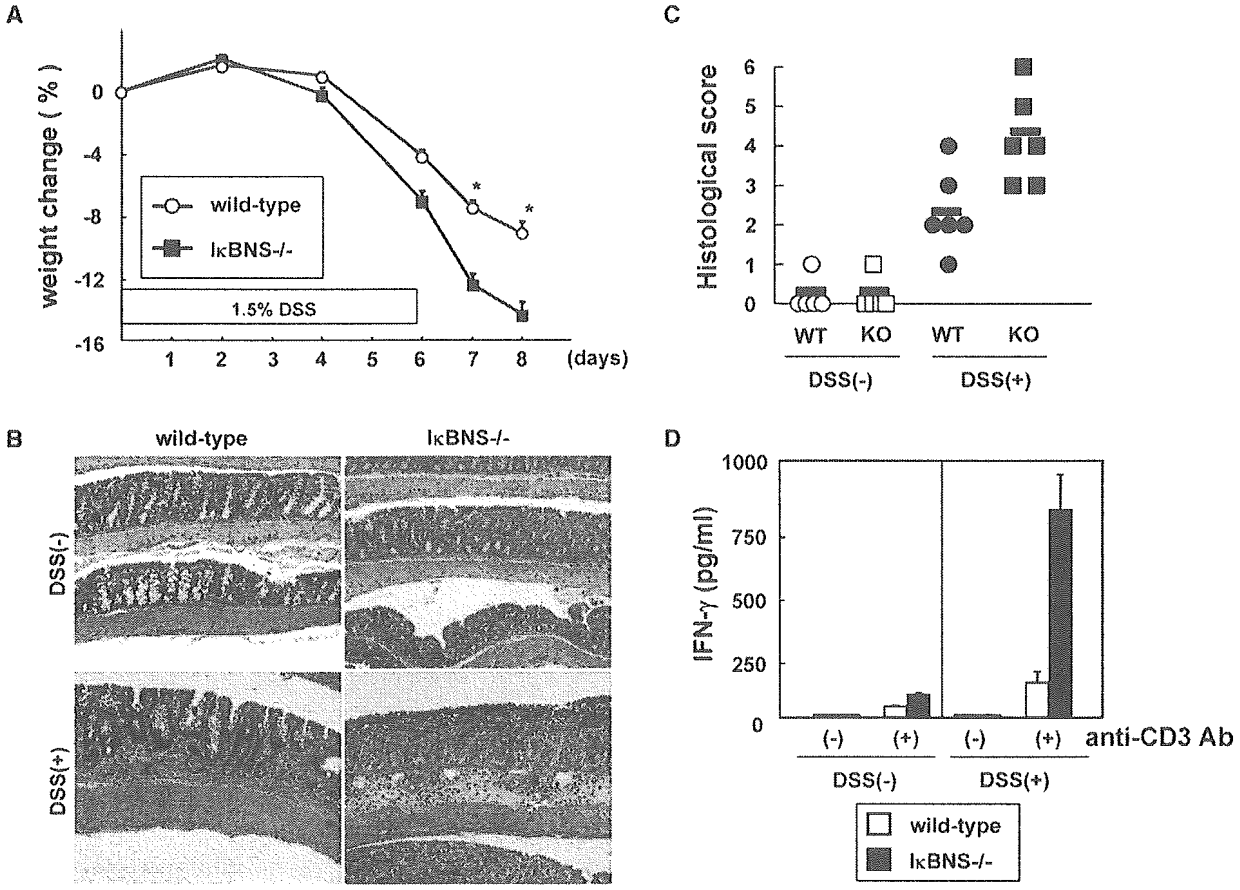

Figure 7. High Susceptibility to DSS Colitis in IκBNS$^{-/-}$ Mice

(A) Wild-type (n = 15) and IκBNS$^{-/-}$ mice (n = 15) were given 1.5% DSS in drinking water for 6 days and weighed everyday. Data are mean ± SD. *, $p < 0.05$.

(B) Histologic examination of the colons of wild-type and IκBNS$^{-/-}$ mice before or 9 days after initiation of DSS administration. H&E staining is shown. Representative of six mice examined. Magnification, 20×.

(C) The colitis scores shown for individual wild-type (circle) and IκBNS$^{-/-}$ mice (square) before (open) and after (closed) DSS treatment were total scores for individual sections as described in the Experimental Procedures section. Mean score for each group is also shown (black bar).

(D) CD4$^+$ T cells were purified from spleen of wild-type or IκBNS$^{-/-}$ mice either treated or nontreated with DSS. Then, CD4$^+$ T cells were cultured in the presence or absence of plate bound anti-CD3 Ab for 24 hr. Concentration of IFN-γ in the culture supernatants was measured by ELISA.

So far, characterized negative regulators are mainly involved in blockade of TLR signaling pathways in the cytoplasm or on the cell membrane. Accordingly, these negative regulators globally inhibit TLR-dependent gene induction. The nuclear IκB protein IκBNS is unique in that this molecule negatively regulates induction of a set of TLR-dependent genes by directly affecting NF-κB activity in the nucleus. Thus, TLR-dependent innate immune responses are regulated through a variety of mechanisms.

IκBNS-mediated inhibition of a set of TLR-dependent genes is probably explained by recruitment of IκBNS to the specific promoters. IκBNS was recruited to the IL-6 promoter, but not to the TNF-α promoter. In addition, LPS-induced recruitment of p65 to the TNF-α promoter was observed within 1 hr, whereas p65 recruitment to the IL-6 promoter was observed late, indicating that NF-κB activity was differentially regulated at both promoters. NF-κB activity at the TNF-α promoter is regulated in an IκBNS-independent manner, whereas the activity at the IL-6 promoter was IκBNS-dependent. Indeed, p65 recruitment to the TNF-α promoter was observed similarly in wild-type and IκBNS$^{-/-}$ macrophages, but the recruitment to the IL-6 promoter was sustained in IκBNS$^{-/-}$ cells. Previous reports indicate that IκBNS selectively associates with p50 subunit of NF-κB and affects NF-κB DNA binding activity (Fiorini et al., 2002; Hirotani et al., 2005). Consistent with these observations, IκBNS$^{-/-}$ macrophages showed prolonged LPS-induced NF-κB DNA binding activity and nuclear localization of p65. Taken together, these findings indicate that IκBNS, which is rapidly induced by TLR stimulation, might be recruited to gene promoters through association with p50, and contribute to termination of NF-κB activity. Termination of NF-κB activity has been shown to be induced by IKKα-mediated degradation of promoter-bound p65 (Lawrence et al., 2005). However, consistent with a recent report, we were not able to detect LPS-induced degradation of p65 in peritoneal macrophages and bone marrow-derived macrophages (Li et al., 2005). However, we could detect LPS-induced p65 degradation in the RAW264.7 macrophage cell line. In these cells, when constitutively expressed IκBNS, LPS-induced p65 turnover was

accelerated, indicating that IκBNS is involved in the degradation of promoter-bound p65. In the case of the TNF-α promoter, it is possible that NF-κB activity is already terminated when IκBNS expression is induced, and therefore IκBNS is no longer recruited to the TNF-α promoter. Alternatively, an unidentified mechanism that regulates selective recruitment of IκBNS to gene promoters might exist. The mechanisms by which IκBNS is recruited to the specific promoters through association with p50 remain unclear and would be a subject of further investigation.

Analyses of IκBNS$^{-/-}$ mice further highlighted the in vivo functions of IκBNS in limiting systemic and intestinal inflammation. IκBNS$^{-/-}$ mice succumbed to systemic LPS-induced endotoxin shock possibly due to sustained production of several TLR-dependent gene products such as IL-6 and IL-12p40. Furthermore, IκBNS$^{-/-}$ mice are more susceptible to intestinal inflammation induced by disruption of the epithelial barrier. Abnormal activation of innate immune cells caused by deficiency of IL-10 or Stat3 leads to spontaneous development of colonic inflammation (Kobayashi et al., 2003; Kuhn et al., 1993; Takeda et al., 1999). IκBNS$^{-/-}$ mice did not develop chronic colitis spontaneously until 20 week-old of age (our unpublished data). In Stat3 mutant mice, TLR-dependent production of proinflammatory cytokines increased over 10-fold compared to wild-type cells, which might contribute to the spontaneous intestinal inflammation (Takeda et al., 1999). In IκBNS$^{-/-}$ mice, increase in TLR-dependent production of proinflammatory cytokines such as IL-6 and IL-12p40 was mild compared to Stat3 mutant mice. In this case, the colonic epithelial barrier might contribute to prevention of excessive inflammatory responses in IκBNS$^{-/-}$ mice. However, when the barrier function of epithelial cells was disrupted by administration of DSS, IκBNS$^{-/-}$ mice suffered from severe intestinal inflammation accompanied by enhanced Th1 responses. IκBNS was shown to be expressed in CD11b^{+} cells residing in the colonic lamina propria (Hirotani et al., 2005). Therefore, in the absence of IκBNS, exposure of innate immune cells to intestinal microflora might result in increased or sustained production of proinflammatory cytokines such as IL-12p40, which induces exaggerated intestinal inflammation and Th1 cell development. Thus, IκBNS is responsible for the prevention of uncontrolled inflammatory responses in vivo.

In this study, we have shown that IκBNS is a selective inhibitor of TLR-dependent genes possibly through termination of NF-κB activity. Furthermore, IκBNS was responsible for prevention of inflammation through inhibition of persistent proinflammatory cytokine production. Future study that discloses the precise molecular mechanisms by which the nuclear IκB protein selectively inhibits TLR-dependent genes will provide basis for the development of new therapeutic strategies to a variety of inflammatory diseases.

Experimental Procedures

Generation of IκBNS-Deficient Mice

The *Ikbns* gene consists of eight exons (Figure 1A). The targeting vector was designed to replace a 1.8 kb fragment containing exons 5–8 of the *Ikbns* gene with a neomycin-resistance gene (*neo*). A short arm and a long arm of the homology region from the E14.1 ES genome were amplified by PCR. A herpes simplex virus thymidine kinase gene (HSV-TK) was inserted into the 3′ end of the vector. After the targeting vector was electroporated into ES cells, G418 and gancyclovir doubly resistant clones were selected and screened for homologous recombination by PCR and verified by Southern blot analysis using the probe indicated in Figure 1A. Two independently identified targeted ES clones were microinjected into C57BL/6 blastocysts. Chimeric mice were mated with C57BL/6 female mice, and heterozygous F1 progenies were intercrossed to obtain IκBNS$^{-/-}$ mice. Mice from these independent ES clones displayed identical phenotypes. All animal experiments were conducted according to guidelines of Animal Care and Use Committee at Kyushu University.

Reagents

LPS (*E. coli* 055:B5) was purchased from Sigma. Peptidoglycan was from Fluca. Pam_3CSK_4, MALP-2, and imiquimod were from Invivogen. Antibodies against p65 (C-20; sc-372), p50 (H-119; sc-7178 or NLS; sc-114), c-Rel (C; sc-71), and RNA polymerase II (H-224; sc-9001) were purchased from Santa Cruz. Rabbit anti-IκBNS Ab was generated against synthetic peptide (1-MEDSLDTRLY PEPSLSQVC-18) corresponding to N-terminal region of mouse IκBNS (MBL, Nagoya, Japan), and anti-IκBNS serum was affinity-purified using a column containing peptide-conjugated Sepharose 4B.

Preparation of Macrophages and Dendritic Cells

For isolation of peritoneal macrophages, mice were intraperitoneally injected with 2 ml of 4% thioglycollate medium (Sigma). Peritoneal exudate cells were isolated from the peritoneal cavity 3 days post injection. Cells were incubated for 2 hr and washed three times with HBSS. Remaining adherent cells were used as peritoneal macrophages for the experiments. To prepare bone marrow-derived macrophages, bone marrow cells were prepared from femora and tibia and passed through nylon mesh. Then cells were cultured in RPMI 1640 medium supplemented with 10% FCS, 100 μM 2-ME, and 10 ng/ml M-CSF (GenzymeTechne). After 6–8 days, the cells were used as macrophages for the experiments. Bone marrow-derived DCs were prepared by culturing bone marrow cells in RPMI 1640 medium supplemented with 10% FCS, 100 μM 2-ME, and 10 ng/ml GM-CSF (GenzymeTechne). After 6 days, the cells were used as DCs.

Measurement of Cytokine Production

Peritoneal macrophages or DCs were stimulated with various TLR ligands for 24 hr. Culture supernatants were collected and analyzed for TNF-α, IL-6, IL-12p40, IL-12p70, or IL-10 production with enzyme-linked immunosorbent assay (ELISA). Mice were intravenously injected with 1mg of LPS and bled at the indicated periods. Serum concentrations of TNF-α, IL-6, and IL-12p40 were determined by ELISA. ELISA kits were purchased from GenzymeTechne and R&D Systems. For measurement of IFN-γ, CD4^{+} T cells were purified from spleen cells using CD4 microbeads (Miltenyi Biotec) and stimulated by plate bound anti-CD3ε antibody (145-2C11, BD PharMingen) for 24 hr. Concentrations of IFN-γ in the supernatants were determined by ELISA (GenzymeTechne).

Quantitative Real-Time RT-PCR

Total RNA was isolated with TRIzol reagent (Invitrogen, Carlsbad, CA), and 2 μg of RNA was reverse transcribed using M-MLV reverse transcriptase (Promega, Madison, WI) and oligo (dT) primers (Toyobo, Osaka, Japan) after treatment with RQ1 DNase I (Promega). Quantitative real-time PCR was performed on an ABI 7700 (Applied Biosystems, Foster City, CA) using TaqMan Universal PCR Master Mix (Applied Biosystems). All data were normalized to the corresponding elongation factor-1α (EF-1α) expression, and the fold difference relative to the EF-1α level was shown. Amplification conditions were: 50°C (2 min), 95°C (10 min), 40 cycles of 95°C (15 s), and 60°C (60 s). Each experiment was performed independently at least three times, and the results of one representative experiment are shown. All primers were purchased from Assay on Demand (Applied Biosystems).

Electrophoretic Mobility Shift Assay

Macrophages were stimulated with 100 ng/ml LPS for the indicated periods. Then, nuclear proteins were extracted, and incubated with an end-labeled, double-stranded oligonucleotide containing an NF-κB binding site of the IL-6 promoter in 25 μl of binding buffer (10 mM HEPES-KOH, [pH 7.8], 50 mM KCl, 1 mM EDTA [pH 8.0], 5 mM $MgCl_2$ and 10% glycerol) for 20 min at room temperature and loaded on a native 5% polyacrylamide gel. The DNA-protein complexes were visualized by autoradiography.

Western Blotting

Cells were lysed with RIPA buffer (50 mM Tris-HCl [pH 7.5], 150 mM NaCl, 1% Triton X-100, 0.5% Na-deoxycholate) containing protease inhibitors (Complete Mini; Roche). The lysates were separated on SDS-PAGE and transferred to PVDF membrane. The membranes were incubated with anti-IκBα Ab, anti-ERK Ab, anti-p38 Ab, anti-JNK Ab (Santa Cruz Biotechnology), anti-phospho-p38 Ab, anti-phospho-ERK Ab, or anti-phospho-JNK Ab (Cell Signaling Technology). Bound Abs were detected with SuperSignal West Pico Chemiluminescent Substrate (Pierce).

Immunofluorescence Staining

Macrophages were stimulated with 100 ng/ml LPS for the indicated periods, washed with Tris-buffered saline (TBS), and fixed with 3.7% formaldehyde in TBS for 15 min at room temperature. After permeabilization with 0.2% Triton X-100, cells were washed with TBS and incubated with 10 ng/ml of a rabbit anti-p50 or anti-p65 Ab (Santa Cruz Biotechnology) in TBS containing 1% bovine serum albumin, followed by incubation with Alexa Fluor 594-conjugated goat anti-rabbit immunoglobulin G (IgG; Molecular Probes, Eugene, OR). To stain the nucleus, cells were cultured with 0.5 μg/ml 4, 6-diamidino-2-phenylindole (DAPI; Wako, Osaka, Japan). Stained cells were analyzed using an LSM510 model confocal microscope (Carl Zeiss, Oberkochem, Germany).

Chromatin Immunoprecipitation

Chromatin immunoprecipitation (ChIP) was performed essentially with a described protocol (Upstate Biotechnology, Lake Placid, NY). In brief, peritoneal macrophages from wild-type and $I\kappa BNS^{-/-}$ mice were stimulated with 100 ng/ml LPS for 1, 3, or 5 hr, and then fixed with formaldehyde for 10 min. The cells were lysed, sheared by sonication using Bioruptor (CosmoBio), and incubated overnight with specific antibody followed by incubation with protein A-agarose saturated with salmon sperm DNA (Upsate Biotechnology). Precipitated DNA was analyzed by quantitative PCR (35 cycles) using primers 5′- CCCCAGATTGCCACAGAATC -3′ and 5′- CCAGT GAGTGAAAGGGACAG -3′ for the TNF-α promoter and 5′- TGTGTG TCGTCTGTCATGCG-3′ and 5′- AGCTACAGACATCCCCAGTCTC -3′ for the IL-6 promoter.

Induction of DSS Colitis

Mice received 1.5% (wt/vol) DSS (40,000 kDa; ICN Biochemicals), ad libitum, in their drinking water for 6 days, then switched to regular drinking water. The amount of DSS water drank per animal was recorded and no differences in intake between strains were observed. Mice were weighed for the determination of percent weight change. This was calculated as: percentage weight change = (weight at day X-day 0/weight at day 0) × 100. Statistical significance was determined by paired Student's t test. Differences were considered to be statistically significant at $p < 0.05$.

Histological Analysis

Colon tissues were fixed in 4% paraformaldehyde, rolled up, and embedded in paraffin in a Swiss roll orientation such that the entire length of the intestinal tract could be identified on single sections. After sectioning, the tissues were dewaxed in ethanol, rehydrated, and stained hematoxylin and eosin to study histological changes after DSS-induced damage. Histological scoring was performed in a blinded fashion by a pathologist, with a combined score for inflammatory cell infiltration (score, 0–3) and tissue damage (score, 0–3) (Araki et al., 2005). The presence of occasional inflammatory cells in the lamina propria was assigned a value of 0; increased numbers of inflammatory cells in the lamina propria as 1; confluence of inflammatory cells, extending into the submucosa, as 2; and transmural extension of the infiltrate as 3. For tissue damage, no mucosal damage was scored as 0; discrete lymphoepithelial lesions were scored as 1; surface mucosal erosion or focal ulceration was scored as 2; and extensive mucosal damage and extension into deeper structures of the bowel wall were scored as 3. The combined histological score ranged from 0 (no changes) to 6 (extensive cell infiltration and tissue damage).

Supplemental Data

Supplemental Data include four figures and are available with this article online at http://www.immunity.com/cgi/content/full/24/1/41/DC1/.

Acknowledgments

We thank Y. Yamada, K. Takeda, M. Otsu, and N. Kinoshita for technical assistance; M. Yamamoto and S. Akira for providing us with reagents, P. Lee for critical reading of the manuscript, and M. Kurata for secretarial assistance. This work was supported by grants from the Special Coordination Funds of the Ministry of Education, Culture, Sports, Science and Technology; the Uehara Memorial Foundation; the Mitsubishi Foundation; the Takeda Science Foundation; the Tokyo Biochemical Research Foundation; the Kowa Life Science Foundation; the Osaka Foundation for Promotion of Clinical Immunology; and the Sankyo Foundation of Life Science.

Received: July 15, 2005
Revised: September 16, 2005
Accepted: November 16, 2005
Published: January 17, 2006

References

Akira, S., and Takeda, K. (2004). Toll-like receptor signalling. Nat. Rev. Immunol. *4*, 499–511.

Araki, A., Kanai, T., Ishikura, T., Makita, S., Uraushihara, K., Iiyama, R., Totsuka, T., Takeda, K., Akira, S., and Watanabe, M. (2005). MyD88-deficient mice develop severe intestinal inflammation in dextran sodium sulfate colitis. J. Gastroenterol. *40*, 16–23.

Beutler, B. (2004). Inferences, questions and possibilities in Toll-like receptor signalling. Nature *430*, 257–263.

Bjorkbacka, H., Kunjathoor, V.V., Moore, K.J., Koehn, S., Ordija, C.M., Lee, M.A., Means, T., Halmen, K., Luster, A.D., Golenbock, D.T., and Freeman, M.W. (2004). Reduced atherosclerosis in MyD88-null mice links elevated serum cholesterol levels to activation of innate immunity signaling pathways. Nat. Med. *10*, 416–421.

Boone, D.L., Turer, E.E., Lee, E.G., Ahmad, R.C., Wheeler, M.T., Tsui, C., Hurley, P., Chien, M., Chai, S., Hitotsumatsu, O., et al. (2004). The ubiquitin-modifying enzyme A20 is required for termination of Toll-like receptor responses. Nat. Immunol. *5*, 1052–1060.

Brint, E.K., Xu, D., Liu, H., Dunne, A., McKenzie, A.N., O'Neill, L.A., and Liew, F.Y. (2004). ST2 is an inhibitor of interleukin 1 receptor and Toll-like receptor 4 signaling and maintains endotoxin tolerance. Nat. Immunol. *5*, 373–379.

Burns, K., Janssens, S., Brissoni, B., Olivos, N., Beyaert, R., and Tschopp, J. (2003). Inhibition of interleukin 1 receptor/Toll-like receptor signaling through the alternatively spliced, short form of MyD88 is due to its failure to recruit IRAK-4. J. Exp. Med. *197*, 263–268.

Chuang, T.H., and Ulevitch, R.J. (2004). Triad3A, an E3 ubiquitin-protein ligase regulating Toll-like receptors. Nat. Immunol. *5*, 495–502.

Diehl, G.E., Yue, H.H., Hsieh, K., Kuang, A.A., Ho, M., Morici, L.A., Lenz, L.L., Cado, D., Riley, L.W., and Winoto, A. (2004). TRAIL-R as a negative regulator of innate immune cell responses. Immunity *21*, 877–889.

Divanovic, S., Trompette, A., Atabani, S.F., Madan, R., Golenbock, D.T., Visintin, A., Finberg, R.W., Tarakhovsky, A., Vogel, S.N., Belkaid, Y., et al. (2005). Negative regulation of Toll-like receptor 4 signaling by the Toll-like receptor homolog RP105. Nat. Immunol. *6*, 571–578.

Eriksson, U., Ricci, R., Hunziker, L., Kurrer, M.O., Oudit, G.Y., Watts, T.H., Sonderegger, I., Bachmaier, K., Kopf, M., and Penninger, J.M.

(2003). Dendritic cell-induced autoimmune heart failure requires cooperation between adaptive and innate immunity. Nat. Med. *9*, 1484–1490.

Fiorini, E., Schmitz, I., Marissen, W.E., Osborn, S.L., Touma, M., Sasada, T., Reche, P.A., Tibaldi, E.V., Hussey, R.E., Kruisbeek, A.M., et al. (2002). Peptide-induced negative selection of thymocytes activates transcription of an NF-kappa B inhibitor. Mol. Cell *9*, 637–648.

Fukao, T., Tanabe, M., Terauchi, Y., Ota, T., Matsuda, S., Asano, T., Kadowaki, T., Takeuchi, T., and Koyasu, S. (2002). PI3K-mediated negative feedback regulation of IL-12 production in DCs. Nat. Immunol. *3*, 875–881.

Hirotani, T., Lee, P.Y., Kuwata, H., Yamamoto, M., Matsumoto, M., Kawase, I., Akira, S., and Takeda, K. (2005). The nuclear IkappaB protein IkappaBNS selectively inhibits lipopolysaccharide-induced IL-6 production in macrophages of the colonic lamina propria. J. Immunol. *174*, 3650–3657.

Honda, K., Yanai, H., Negishi, H., Asagiri, M., Sato, M., Mizutani, T., Shimada, N., Ohba, Y., Takaoka, A., Yoshida, N., and Taniguchi, T. (2005). IRF-7 is the master regulator of type-I interferon-dependent immune responses. Nature *434*, 772–777.

Iwasaki, A., and Medzhitov, R. (2004). Toll-like receptor control of the adaptive immune responses. Nat. Immunol. *5*, 987–995.

Kawai, T., Adachi, O., Ogawa, T., Takeda, K., and Akira, S. (1999). Unresponsiveness of MyD88-deficient mice to endotoxin. Immunity *11*, 115–122.

Kinjyo, I., Hanada, T., Inagaki-Ohara, K., Mori, H., Aki, D., Ohishi, M., Yoshida, H., Kubo, M., and Yoshimura, A. (2002). SOCS1/JAB is a negative regulator of LPS-induced macrophage activation. Immunity *17*, 583–591.

Kisielow, P., Bluthmann, H., Staerz, U.D., Steinmetz, M., and von Boehmer, H. (1988). Tolerance in T-cell-receptor transgenic mice involves deletion of nonmature CD4+8+ thymocytes. Nature *333*, 742–746.

Kitajima, S., Takuma, S., and Morimoto, M. (1999). Changes in colonic mucosal permeability in mouse colitis induced with dextran sulfate sodium. Exp. Anim. *48*, 137–143.

Kobayashi, K., Hernandez, L.D., Galan, J.E., Janeway, C.A., Jr., Medzhitov, R., and Flavell, R.A. (2002). IRAK-M is a negative regulator of Toll-like receptor signaling. Cell *110*, 191–202.

Kobayashi, M., Kweon, M.N., Kuwata, H., Schreiber, R.D., Kiyono, H., Takeda, K., and Akira, S. (2003). Toll-like receptor-dependent production of IL-12p40 causes chronic enterocolitis in myeloid cell-specific Stat3-deficient mice. J. Clin. Invest. *111*, 1297–1308.

Kuhn, R., Lohler, J., Rennick, D., Rajewsky, K., and Muller, W. (1993). Interleukin-10-deficient mice develop chronic enterocolitis. Cell *75*, 263–274.

Kuwata, H., Watanabe, Y., Miyoshi, H., Yamamoto, M., Kaisho, T., Takeda, K., and Akira, S. (2003). IL-10-inducible Bcl-3 negatively regulates LPS-induced TNF-alpha production in macrophages. Blood *102*, 4123–4129.

Lang, K.S., Recher, M., Junt, T., Navarini, A.A., Harris, N.L., Freigang, S., Odermatt, B., Conrad, C., Ittner, L.M., Bauer, S., et al. (2005). Toll-like receptor engagement converts T-cell autoreactivity into overt autoimmune disease. Nat. Med. *11*, 138–145.

Lawrence, T., Bebien, M., Liu, G.Y., Nizet, V., and Karin, M. (2005). IKKalpha limits macrophage NF-kappaB activation and contributes to the resolution of inflammation. Nature *434*, 1138–1143.

Leadbetter, E.A., Rifkin, I.R., Hohlbaum, A.M., Beaudette, B.C., Shlomchik, M.J., and Marshak-Rothstein, A. (2002). Chromatin-IgG complexes activate B cells by dual engagement of IgM and Toll-like receptors. Nature *416*, 603–607.

Li, Q., Lu, Q., Bottero, V., Estepa, G., Morrison, L., Mercurio, F., and Verma, I.M. (2005). Enhanced NF-(kappa)B activation and cellular function in macrophages lacking I(kappa)B kinase 1 (IKK1). Proc. Natl. Acad. Sci. USA *102*, 12425–12430.

Liew, F.Y., Xu, D., Brint, E.K., and O'Neill, L.A. (2005). Negative regulation of Toll-like receptor-mediated immune responses. Nat. Rev. Immunol. *5*, 446–458.

Michelsen, K.S., Wong, M.H., Shah, P.K., Zhang, W., Yano, J., Doherty, T.M., Akira, S., Rajavashisth, T.B., and Arditi, M. (2004). Lack of Toll-like receptor 4 or myeloid differentiation factor 88 reduces atherosclerosis and alters plaque phenotype in mice deficient in apolipoprotein E. Proc. Natl. Acad. Sci. USA *101*, 10679–10684.

Moore, K.W., de Waal Malefyt, R., Coffman, R.L., and O'Garra, A. (2001). Interleukin-10 and the interleukin-10 receptor. Annu. Rev. Immunol. *19*, 683–765.

Motoyama, M., Yamazaki, S., Eto-Kimura, A., Takeshige, K., and Muta, T. (2005). Positive and negative regulation of nuclear factor-kappaB-mediated transcription by IkappaB-zeta, an inducible nuclear protein. J. Biol. Chem. *280*, 7444–7451.

Nakagawa, R., Naka, T., Tsutsui, H., Fujimoto, M., Kimura, A., Abe, T., Seki, E., Sato, S., Takeuchi, O., Takeda, K., et al. (2002). SOCS-1 participates in negative regulation of LPS responses. Immunity *17*, 677–687.

Natoli, G., Saccani, S., Bosisio, D., and Marazzi, I. (2005). Interactions of NF-kappaB with chromatin: the art of being at the right place at the right time. Nat. Immunol. *6*, 439–445.

Pasare, C., and Medzhitov, R. (2004). Toll-dependent control mechanisms of CD4 T cell activation. Immunity *21*, 733–741.

Saccani, S., Marazzi, I., Beg, A.A., and Natoli, G. (2004). Degradation of promoter-bound p65/RelA is essential for the prompt termination of the nuclear factor kappaB response. J. Exp. Med. *200*, 107–113.

Sakaguchi, S., Negishi, H., Asagiri, M., Nakajima, C., Mizutani, T., Takaoka, A., Honda, K., and Taniguchi, T. (2003). Essential role of IRF-3 in lipopolysaccharide-induced interferon-beta gene expression and endotoxin shock. Biochem. Biophys. Res. Commun. *306*, 860–866.

Strober, W., Fuss, I.J., and Blumberg, R.S. (2002). The immunology of mucosal models of inflammation. Annu. Rev. Immunol. *20*, 495–549.

Takaoka, A., Yanai, H., Kondo, S., Duncan, G., Negishi, H., Mizutani, T., Kano, S., Honda, K., Ohba, Y., Mak, T.W., and Taniguchi, T. (2005). Integral role of IRF-5 in the gene induction programme activated by Toll-like receptors. Nature *434*, 243–249.

Takeda, K., Clausen, B.E., Kaisho, T., Tsujimura, T., Terada, N., Forster, I., and Akira, S. (1999). Enhanced Th1 activity and development of chronic enterocolitis in mice devoid of Stat3 in macrophages and neutrophils. Immunity *10*, 39–49.

Wald, D., Qin, J., Zhao, Z., Qian, Y., Naramura, M., Tian, L., Towne, J., Sims, J.E., Stark, G.R., and Li, X. (2003). SIGIRR, a negative regulator of Toll-like receptor-interleukin 1 receptor signaling. Nat. Immunol. *4*, 920–927.

Wessells, J., Baer, M., Young, H.A., Claudio, E., Brown, K., Siebenlist, U., and Johnson, P.F. (2004). BCL-3 and NF-kappaB p50 attenuate lipopolysaccharide-induced inflammatory responses in macrophages. J. Biol. Chem. *279*, 49995–50003.

Yamamoto, M., Sato, S., Hemmi, H., Hoshino, K., Kaisho, T., Sanjo, H., Takeuchi, O., Sugiyama, M., Okabe, M., Takeda, K., and Akira, S. (2003). Role of adaptor TRIF in the MyD88-independent toll-like receptor signaling pathway. Science *301*, 640–643.

Yamamoto, M., Yamazaki, S., Uematsu, S., Sato, S., Hemmi, H., Hoshino, K., Kaisho, T., Kuwata, H., Takeuchi, O., Takeshige, K., et al. (2004). Regulation of Toll/IL-1-receptor-mediated gene expression by the inducible nuclear protein IkappaBzeta. Nature *430*, 218–222.

nature immunology

Essential function for the kinase TAK1 in innate and adaptive immune responses

Shintaro Sato[1,7], Hideki Sanjo[2,3,7], Kiyoshi Takeda[4], Jun Ninomiya-Tsuji[5], Masahiro Yamamoto[2], Taro Kawai[1], Kunihiro Matsumoto[6], Osamu Takeuchi[1,2] & Shizuo Akira[1,2]

Transforming growth factor-β–activated kinase 1 (TAK1) has been linked to interleukin 1 receptor and tumor necrosis factor receptor signaling. Here we generated mouse strains with conditional expression of a *Map3k7* allele encoding part of TAK1. TAK1-deficient embryonic fibroblasts demonstrated loss of responses to interleukin 1β and tumor necrosis factor. Studies of mice with B cell–specific TAK1 deficiency showed that TAK1 was indispensable for cellular responses to Toll-like receptor ligands, CD40 and B cell receptor crosslinking. In addition, antigen-induced immune responses were considerably impaired in mice with B cell–specific TAK1 deficiency. TAK1-deficient cells failed to activate transcription factor NF-κB and mitogen-activated protein kinases in response to interleukin 1β, tumor necrosis factor and Toll-like receptor ligands. However, TAK1-deficient B cells were able to activate NF-κB but not the kinase Jnk in response to B cell receptor stimulation. These results collectively indicate that TAK1 is key in the cellular response to a variety of stimuli.

Proinflammatory cytokines such as tumor necrosis factor (TNF) and interleukin 1β (IL-1β) have a critical function in innate immune responses by eliciting inflammation[1,2]. The production of proinflammatory cytokines can be induced by various cellular stresses, including pathogenic infection. The initial recognition of invading pathogens is mediated by Toll-like receptors (TLRs), which detect distinct pathogen-associated molecular patterns[2–4]. Stimulation of cells with TLR ligands, IL-1β and TNF activates intracellular signaling pathways leading to the activation of transcription factors such as NF-κB and AP-1 (ref. 1). Activation of AP-1 is mediated by mitogen-activated protein kinases (MAPKs), including Erk, Jnk and p38. Ultimately, these transcription factors initiate expression of genes involved in inflammatory responses. It is well known that TLRs and IL-1 receptor (IL-1R) activate similar signaling pathways[3]. The cytoplasmic portions of TLRs and IL-1Rs contain the Toll–IL-1R homology domain. Ligand stimulation recruits MyD88, a Toll–IL-1R homology domain–containing adaptor protein, to the Toll–IL-1R homology domain of the receptor. Subsequently, IL-1R-associated kinases (IRAKs) are recruited and phosphorylated, and then they interact with TNF receptor (TNFR)–associated factor 6 (TRAF6)[3]. TRAF6 comprises an N-terminal RING finger domain, which has been found in a family of E3 ubiquitin ligases[5]. It has been proposed that a dimeric ubiquitin-conjugating enzyme complex composed of Ubc13 and Uev1A, together with TRAF6, can catalyze the formation of a K63-linked polyubiquitin chain[5,6]. The ubiquitination is responsible for the activation of IκB kinases (IKKs). Subsequently, phosphorylated IκB undergoes degradation by the ubiquitin-proteosome system, and NF-κB translocates into nucleus and triggers transcription of target genes[7]. Simultaneously, MAPKs are activated 'downstream' of TRAF6 by activating MAPK kinase 6 (MKK6)[8]. In the TNFR signaling pathway, ligand stimulation leads to the recruitment of adaptor proteins, including TRADD, TRAF2 and RIP1, to the receptor complex. Genetic studies have shown that TRAF2 is responsible for MAPK activation, whereas RIP1 is required for NF-κB activation[1,4].

Transforming growth factor-β–activated kinase 1 (TAK1), a member of the MAPK kinase kinase (MAPKKK) family, was originally identified as a kinase involved in TGF-β signaling[9]. TAK1 is evolutionally conserved, and drosophila TAK1 is critical for antibacterial innate immunity[10]. In addition, TAK1 functions as an 'upstream' signaling molecule of NF-κB and MAPKs in IL-1R signaling pathways. Furthermore, TAK1 is activated by TNF, bacterial lipopolysaccharide (LPS) and latent membrane protein 1 from Epstein-Barr virus[11–13]. Activated TAK1 is recruited to TRAF6 and TRAF2 complexes in response to IL-1R and TNFR stimulation, respectively. A point mutation in the gene encoding TAK1 altering its ATP-binding domain abolishes both its kinase activity and its ability to activate IKKs and MAPKs[8]. TAK1 forms a complex with its association partners, TAB1, TAB2 and TAB3 (refs. 14–17). It has been proposed that TRAF6-mediated K63-linked

[1]Akira Innate Immunity Project, Exploratory Research for Advanced Technology, Japan Science and Technology Agency and [2]Department of Host Defense, Research Institute for Microbial Diseases, Osaka University, Suita, Osaka 565-0871, Japan. [3]Lymphocyte Differentiation, RIKEN Research Center for Allergy and Immunology, Yokohama, Kanagawa 230-0045, Japan. [4]Department of Molecular Genetics, Medical Institute of Bioregulation, Kyushu University, Fukuoka 812-8582, Japan. [5]Department of Environmental and Molecular Toxicology, North Carolina State University, Raleigh, North Carolina 27695-7633, USA. [6]Department of Molecular Biology, Graduate School of Science, Nagoya University, Nagoya, 464-8602, Japan. [7]These authors contributed equally to this work. Correspondence should be addressed to S.A. (sakira@biken.osaka-u.ac.jp).

Received 4 April; accepted 10 August; published online 25 September 2005; doi:10.1038/ni1255

polyubiquitination is required for the activation of TAK1. Activated TAK1 complex phosphorylates IKKs and MKK6, which activate NF-κB and MAPKs, respectively. *In vitro* studies have shown that expression of TAK1 together with TAB1 enhances activation of a NF-κB reporter gene[8]. Reciprocally, 'knockdown' of *Map3k7*, the gene encoding TAK1, in HeLa cells by RNA interference results in abrogation of IL-1β- and TNF-induced NF-κB activation[11].

The function of TAB1 and TAB2 has been assessed by examination of mouse models lacking genes encoding these proteins. Analysis of TAB2-deficient mice has shown that TAB2 is dispensable for IL-1R signaling[18]. Studies of TAB1-deficient mice have shown that TAB1 is involved in TGF-β signaling[19]. However, the function of TAB1 in IL-1R signaling *in vivo* has not been described. Therefore, it is still unclear whether TAK1-binding proteins are essential for TAK1 activation or if the TAK1 complex itself is dispensable for NF-κB and MAPK signaling *in vivo*. Although the function of TAK1 in drosophila innate immune response has been studied extensively[10], its involvement in the mammalian TLR system is not well understood.

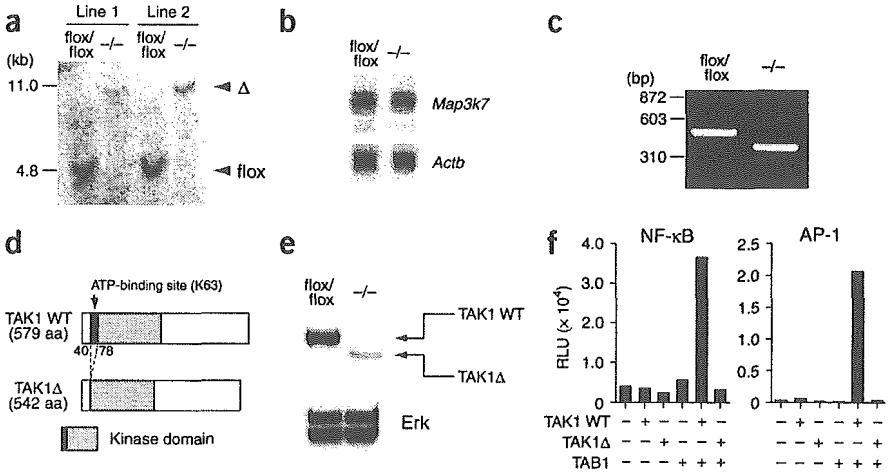

Figure 1 Establishment of *Map3k7*$^{-/-}$ MEFs. (**a**) Southern blot analysis of genomic DNA from *Map3k7*$^{-/-}$ (–/–) and control *Map3k7*$^{flox/flox}$ (flox/flox) MEFs, after digestion with *Xba*I and *Eco*RI (probe, **Supplementary Fig. 1** online). Right and left margins, positions of 11.0-kb floxed and 4.8-kb Δ fragments. (**b**) RNA blot analysis of total RNA prepared from *Map3k7*$^{-/-}$ and *Map3k7*$^{flox/flox}$ MEFs. The 5′ ends of *Map3k7* and *Actb* (encoding β-actin) cDNA fragments were used as probes. (**c**) RT-PCR analysis of total RNA from MEFs, using primers amplifying the encoding region of exons 1–3. (**d**) Predicted structure of TAK1Δ, which lacks the ATP-binding site (arrow) required for kinase activity. WT, wild-type; aa, amino acids. (**e**) Immunoblot analysis of lysates of *Map3k7*$^{-/-}$ and *Map3k7*$^{flox/flox}$ MEFs (antibodies, right margin). (**f**) NF-κB- or AP-1-dependent reporter assay. HEK293 cells were transiently transfected with plasmids (below graphs) plus an NF-κB-dependent (left) or an AP-1-dependent (right) luciferase reporter plasmid. Then, 36 h after transfection, luciferase activity (RLU, relative light units) in whole-cell lysates was measured. Data are representative of three independent experiments.

Here we have examined the function of TAK1 *in vivo* by gene targeting using the Cre-*lox*P system. *Map3k7* deficiency in the germline resulted in early embryonic death. Therefore, we generated TAK1-deficient (*Map3k7*$^{-/-}$) mouse embryonic fibroblasts (MEFs) by *in vitro* introduction of Cre in MEFs homozygous for *lox*P-flanked (floxed) *Map3k7* alleles (*Map3k7*$^{flox/flox}$). First we examined the function of TAK1 in IL-1R and TNF signaling using TAK1-deficient MEFs and found that TAK1 was required for IL-1β- and TNF-induced NF-κB and Jnk activation as well as cytokine production. Next we analyzed TLR- and B cell receptor (BCR)–mediated signaling using B cells as a model. B cell–specific deletion of TAK1 resulted in considerably impaired B cell activation in response to various stimuli, including nonmethylated CpG DNA (a ligand for TLR9), polyinosine-polycytidylic acid (poly(I:C); a ligand for TLR3), LPS (a ligand for TLR4), CD40 and BCR crosslinking. Furthermore, LPS and CpG DNA failed to activate Jnk and NF-κB in TAK1-deficient B cells, indicating that TAK1 is essential for activating these signaling pathways. Notably, although BCR crosslinking on TAK1-deficient B cells also demonstrated defective Jnk activation, activation of NF-κB as well as expression of NF-κB target genes was comparable to that of wild-type cells. Our conditional TAK1-deficient mouse model therefore shows that TAK1 is essential for TLR, IL-1R, TNFR and BCR cellular responses and signaling pathways leading to the activation of Jnk and/or NF-κB.

RESULTS

Map3k7$^{-/-}$ mice die early *in utero*

To investigate the function of TAK1 *in vivo*, we generated mice with conditional deletion of a *Map3k7* allele. We constructed a gene-targeting vector by placing *lox*P sites flanking exon 2 of mouse *Map3k7*, which encodes a part of the kinase domain of TAK1, including its ATP-binding site (Lys63), and a floxed neomycin-resistance gene into an intron 1 of *Map3k7* (**Supplementary Fig. 1** online). To generate mice heterozygous for deletion of this *Map3k7* allele (*Map3k7*$^{+/-}$ mice), we mated mice with one floxed allele and one wild-type allele (*Map3k7*$^{flox/+}$ mice) with a mice of a transgenic line expressing Cre in germ cells. We confirmed deletion of *Map3k7* in the germline by Southern blot analysis (**Supplementary Fig. 1** online). Of about 90 newborn pups obtained by intercrossing *Map3k7*$^{+/-}$ mice, we obtained no *Map3k7*$^{-/-}$ mice, indicating that the TAK1 deficiency is embryonically lethal (**Supplementary Fig. 1** online). Although we identified *Map3k7*$^{-/-}$ embryos on embryonic day 9.5 (E9.5) in normal mendelian ratios, we found no *Map3k7*$^{-/-}$ fetuses in decidua containing normal fetuses after E10.5 (**Supplementary Fig. 1** online).

Establishment of *Map3k7*$^{-/-}$ MEFs

As *Map3k7*$^{-/-}$ MEFs obtained from E9.5 embryos failed to grow, we prepared MEFs from *Map3k7*$^{flox/flox}$ mice. To generate TAK1-deficient MEFs, we excised the floxed genomic fragment by retroviral expression of Cre protein together with green fluorescent protein (GFP). We sorted GFP$^+$ cells by flow cytometry. Southern blot analysis showed that complete conversion of the floxed allele to the deleted (Δ) allele was achieved in GFP$^+$ cells from two lines of *Map3k7*$^{-/-}$ MEFs (**Fig. 1a**). However, we detected *Map3k7* transcripts in *Map3k7*$^{-/-}$ MEFs with same migration and intensity as that of *Map3k7*$^{flox/flox}$ MEFs (**Fig. 1b**). RT-PCR analysis using primers to amplify the region of exons 1–3 showed a product with faster migration in *Map3k7*$^{-/-}$ cells (**Fig. 1c**). Nucleotide sequence analysis of the product showed that the deletion of exon 2 from TAK1 cDNA was in-frame, indicating that Cre-mediated deletion led to the production of an altered TAK1 (TAK1Δ; **Fig. 1d**). Immunoblot analysis showed weak expression of TAK1Δ in *Map3k7*$^{-/-}$ cells (**Fig. 1e**). To confirm that TAK1Δ lacked

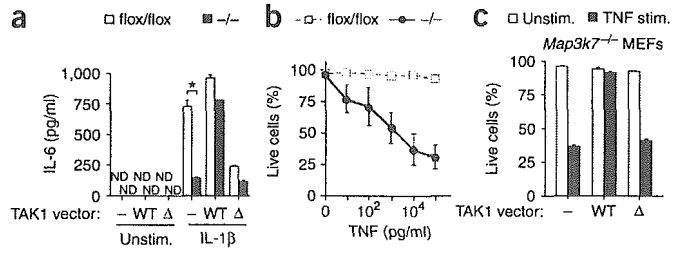

Figure 2 Impaired responses to IL-1β and TNF in *Map3k7*$^{-/-}$ MEFs. (**a**) IL-6 production by MEFs. Control *Map3k7*$^{flox/flox}$ and *Map3k7*$^{-/-}$ MEFs were transfected with empty (–), wild-type TAK1 (WT) or TAK1Δ (Δ) plasmid, and then were stimulated for 24 h with 10 ng/ml of IL-1β. IL-6 in the culture medium was measured by ELISA. Data are mean ± s.d. of triplicate samples of one representative from three independent experiments. *, $P < 0.005$, versus TAK1-deficient cells (Student's *t*-test). ND, not detected. (**b**) Viability of control and *Map3k7*$^{-/-}$ MEFs treated for 24 h with various concentrations of TNF (horizontal axis), assessed by annexin V–indocarbocyanine staining. Three independent experiments were done in triplicate. Data are mean ± s.d. percentage of viable cells after treatment relative to untreated control. (**c**) Viability of control and *Map3k7*$^{-/-}$ MEFs left untransfected or transfected with wild-type or mutated TAK1 and were left unstimulated (Unstim.) or were stimulated for 24 h with 10 ng/ml of TNF (TNF stim.). Data represent mean ± s.d. for percentage of viable cells after treatment relative to untreated control.

the ability to activate NF-κB and AP-1, we did a reporter assay. Overexpression of wild-type TAK1, but not TAK1Δ, together with TAB1 in human embryonic kidney 293 (HEK293) cells activated NF-κB and AP-1, indicating that TAK1Δ was nonfunctional because it lacked an ATP-binding site (**Fig. 1f**).

TAK1 is required for IL-1β and TNF responsiveness

We first examined responses to IL-1β and TNF. We stimulated *Map3k7*$^{-/-}$ and control *Map3k7*$^{flox/flox}$ MEFs with IL-1β and measured IL-6 production by enzyme-linked immunosorbent assay (ELISA). Production of IL-6 was impaired considerably in *Map3k7*$^{-/-}$ MEFs compared with that in control cells (**Fig. 2a**). Moreover, re-expression of wild-type TAK1 but not TAK1Δ in *Map3k7*$^{-/-}$ MEFs restored IL-6 production in response to IL-1β.

As NF-κB activation is required for survival of MEFs after exposure to TNF, we next compared the viability of TNF-stimulated cells. TNF stimulation induced cell death in *Map3k7*$^{-/-}$ MEFs in a dose-dependent way (**Fig. 2b**). In contrast, *Map3k7*$^{flox/flox}$ MEFs were viable after TNF stimulation. The TNF-induced cell death noted in *Map3k7*$^{-/-}$ MEFs was circumvented by expression of wild-type TAK1 but not TAK1Δ (**Fig. 2c**). These results indicate that TAK1 is required for IL-1β- and TNF-mediated cellular responses.

We further examined the activation of signaling molecules. In both *Map3k7*$^{flox/flox}$ and *Map3k7*$^{-/-}$ MEFs, IRAK-1 was phosphorylated, ubiquitinated and degraded in response to IL-1β, indicating that TAK1 was not involved in IRAK-1 activation (**Fig. 3a**). Induction of NF-κB DNA binding and degradation of IκBα in response to IL-1β and TNF were compromised in *Map3k7*$^{-/-}$ MEFs (**Fig. 3b**). Furthermore, activation of Jnk and p38 in response to IL-1β and TNF in *Map3k7*$^{-/-}$ MEFs was also impaired (**Fig. 3c**). Thus, TAK1 was required for NF-κB, Jnk and p38 activation in response to IL-1β and TNF in MEF cells.

Generation of mice with B cell–specific TAK1 deficiency

Although the involvement of TAK1 in the IL-1β signaling has been studied extensively, its involvement in the TLR signaling pathway is less understood. Because B cells express various TLRs and respond to their ligands to proliferate, we generated mice with B cell–specific TAK1 deficiency by breeding *Map3k7*$^{flox/-}$ mice with mice carrying the *Cre* transgene under control of the *Cd19* promoter (*Cd19*$^{Cre/+}$). Southern blot analysis showed almost complete Cre-mediated deletion of *Map3k7* in B cells from *Cd19*$^{Cre/+}$*Map3k7*$^{flox/-}$ mice (**Supplementary Fig. 2** online). We also checked deletion of TAK1 in purified B cells by immunoblot analysis and confirmed that the expression of wild-type TAK1 was considerably reduced in B cells from *Cd19*$^{Cre/+}$*Map3k7*$^{flox/-}$ mice (**Supplementary Fig. 2** online).

TAK1 deficiency impairs B-1 B cell development

We investigated whether B cell–specific TAK1 deficiency affected lymphopoiesis. The population of B cell precursors in the bone marrow was comparable in *Cd19*$^{Cre/+}$*Map3k7*$^{flox/+}$ and *Cd19*$^{Cre/+}$*Map3k7*$^{flox/-}$ mice (**Fig. 4a**). The ratio of B cells to T cells, the expression of surface immunoglobulin M (IgM) and IgD on mature splenic B cells and the numbers of marginal zone B cells ($IgM^+CD23^-CD21^+$) were also comparable for *Cd19*$^{Cre/+}$*Map3k7*$^{flox/+}$ and *Cd19*$^{Cre/+}$*Map3k7*$^{flox/-}$ splenocyte samples (**Fig. 4b**). However, the $B220^+CD5^+$ B-1 B cell population was reduced in the peritoneal cavities of *Cd19*$^{Cre/+}$*Map3k7*$^{flox/-}$ mice (**Fig. 4c**). These results indicate that TAK1 was required for the development of B-1 B cells but not of splenic follicular and marginal zone B cells.

TAK1 is required for the TLR signaling in B cells

B cells become active and progress through the cell cycle in response to TLR ligands such as LPS, CpG DNA and poly(I:C). Although *Cd19*$^{Cre/+}$*Map3k7*$^{flox/+}$ B cells proliferated in response to all TLR

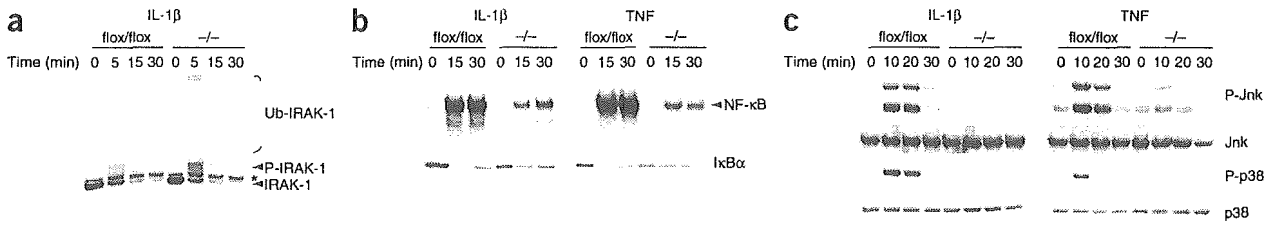

Figure 3 Impaired activation of NF-κB and MAPKs in response to IL-1β and TNF in TAK1-deficient cells. (**a**) Immunoblot of IRAK-1 in whole-cell lysates of control and *Map3k7*$^{-/-}$ MEFs left untreated or treated with 10 ng/ml of IL-1β (time, above lanes). Ub-, ubiquitinated; P-, phosphorylated; *, nonspecific band. (**b**) Control and *Map3k7*$^{-/-}$ MEFs were treated with IL-1β (10 ng/ml) or TNF (10 ng/ml) for various times (above lanes). The NF-κB DNA-binding activity in nuclear extracts was determined by EMSA (top). Degradation of IκBα whole-cell lysates was detected by immunoblot with anti-IκBα (bottom). (**c**) Phosphorylation of Jnk and p38 (P-Jnk and P-p38, respectively) in whole-cell lysates of control and *Map3k7*$^{-/-}$ MEFs treated with IL-1β (10 ng/ml) or TNF (10 ng/ml) for various times (above lanes), assessed by immunoblot with phosphorylation-specific antibodies. Jnk and p38, loading controls. All results are representative of three different experiments.

ligands tested, the proliferation of B cells from *Cd19*$^{Cre/+}$*Map3k7*$^{flox/-}$ mice was considerably impaired (**Fig. 5a**). In addition, follicular and marginal zone B-2 cells purified from *Cd19*$^{Cre/+}$*Map3k7*$^{flox/-}$ spleens had impaired proliferative responses to LPS and/or CpG DNA (**Supplementary Fig. 3** online). We also investigated cell cycle profiles by staining with bromodeoxyuridine (BrdU) and 7-amino-actinomycin D. Unlike *Cd19*$^{Cre/+}$*Map3k7*$^{flox/+}$ B cells, whose cell cycles progressed into S phase, *Cd19*$^{Cre/+}$*Map3k7*$^{flox/-}$ B cells showed impaired entry to S phase after treatment with LPS and CpG DNA (**Fig. 5b**). These results indicate that TAK1 is responsible for TLR-mediated responses in B cells.

We next examined whether TAK1 deficiency influences the viability of B cells. When control B cells were cultured *ex vivo* without mitogens, 50% of the cells spontaneously underwent apoptosis within 12 h of culture (**Fig. 5c**). Stimulation with LPS or CpG DNA prevented the execution of apoptosis in control B cells. In contrast, prevention of cell death in response to LPS or CpG DNA was impaired in *Cd19*$^{Cre/+}$*Map3k7*$^{flox/-}$ B cells. These results indicate that TAK1 is critical for TLR ligand–mediated prevention of B cell death.

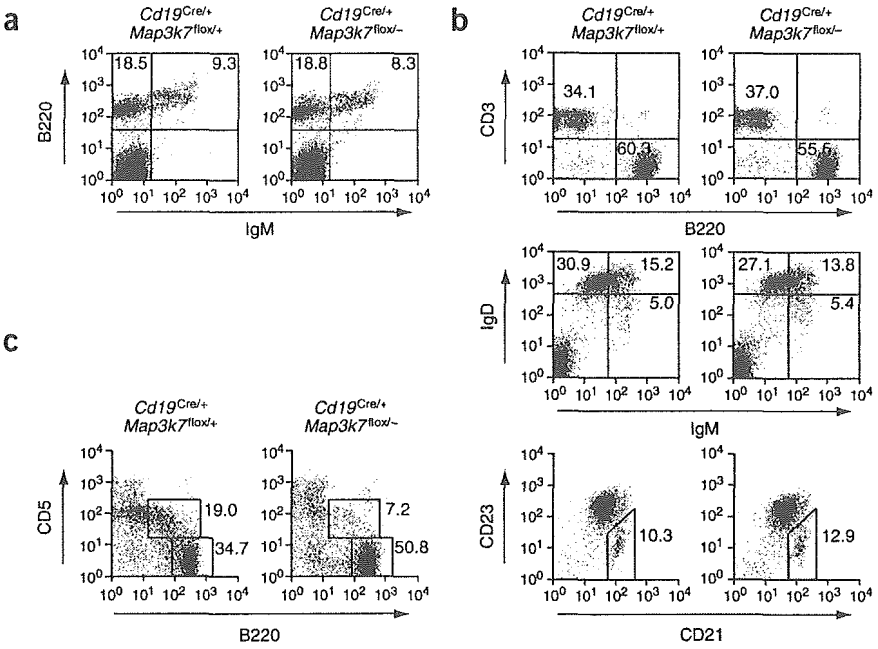

Figure 4 B cell development in *Cd19*$^{Cre/+}$*Map3k7*$^{flox/-}$ mice. Flow cytometry of B cell development in the bone marrow (**a**), splenic (**b**) and peritoneal (**c**) B cells from 8-week-old *Cd19*$^{Cre/+}$*Map3k7*$^{flox/+}$ and *Cd19*$^{Cre/+}$*Map3k7*$^{flox/-}$ mice. Numbers in the quadrants or beside boxed areas indicate the percentage of positive cells in that region. Results are representative of four different experiments.

We further analyzed the upregulation of surface activation markers in response to TLR stimuli. In accordance with defects in cell proliferation and apoptosis inhibition, *Cd19*$^{Cre/+}$*Map3k7*$^{flox/-}$ B cells stimulated with LPS or CpG DNA showed impaired upregulation of cell surface CD69 and CD86 expression (**Fig. 5d**). It has been reported that CpG DNA induces IL-6 production from human naive B cells[20]. In mouse splenic B cells, IL-6 was produced in response to CpG DNA and LPS (**Fig. 5e**). However, IL-6 production by *Cd19*$^{Cre/+}$*Map3k7*$^{flox/-}$ B cells in response to either LPS or CpG DNA was less than that of control *Cd19*$^{Cre/+}$*Map3k7*$^{flox/+}$ B cells.

We also assessed TLR-induced activation of signaling pathways in TAK1-deficient B cells. In *Cd19*$^{Cre/+}$*Map3k7*$^{flox/+}$ B cells, stimulation with LPS or CpG DNA resulted in degradation of IκBα and activation of NF-κB DNA-binding activity (**Fig. 5f,g**). In contrast, IκBα degradation and NF-κB DNA-binding activity in response to LPS and CpG DNA were reduced considerably in *Cd19*$^{Cre/+}$*Map3k7*$^{flox/-}$ B cells. In addition, activation of Jnk, p38 and Erk was impaired in LPS- and CpG DNA–stimulated *Cd19*$^{Cre/+}$*Map3k7*$^{flox/-}$ B cells (**Fig. 5h**). These findings indicate that TAK1 is critical for TLR-mediated B cell activation and signaling.

Requirement for TAK1 for activation of BCR signaling

BCR signaling also activates NF-κB and MAPKs, leading to B cell activation. Crosslinking of BCRs induces activation of tyrosine kinases, an increase in intracellular calcium and activation of protein kinase C-β[21]. A complex of the signaling molecules CARD11 (also known as CARMA1), Bcl10 and MALT1 (also known as paracaspase) then transduces signals to NF-κB and MAPKs downstream of protein kinase C-β[22]. It has also been proposed that TAK1 is involved in T cell receptor signaling downstream of TRAF6 to activate NF-κB[23]. However, the function of TAK1 in BCR signaling is unknown. We therefore analyzed activation of TAK1-deficient B cells in response to BCR crosslinking. Inactivation of TAK1 considerably impaired the proliferation of purified B cells in response to BCR and CD40 stimulation, similar to their response to TLR ligands, indicating that TAK1 is involved in the signaling pathways used by BCRs and CD40 (**Fig. 6a** and **Supplementary Fig. 3** online). Furthermore, *Cd19*$^{Cre/+}$*Map3k7*$^{flox/-}$ B cells showed impaired entry to S phase and impaired enhancement of cell survival after BCR crosslinking compared with that of control *Cd19*$^{Cre/+}$*Map3k7*$^{flox/+}$ B cells (**Fig. 6b,c**). In contrast, BCR stimulation induced almost similar upregulation of CD69 and CD86 in control and *Cd19*$^{Cre/+}$*Map3k7*$^{flox/-}$ B cells (**Fig. 6d**).

We next examined the activation of BCR-mediated signaling pathways in further detail. Tyrosine phosphorylation of cytoplasmic proteins in response to BCR stimulation was not altered in *Cd19*$^{Cre/+}$*Map3k7*$^{flox/-}$ B cells (**Fig. 6e**). Unexpectedly, BCR-mediated activation of NF-κB was not impaired in TAK1-deficient B cells (**Fig. 6f,g**). Among MAPKs, activation of Jnk but not p38 or Erk was considerably impaired (**Fig. 6h**). These data demonstrate that the requirement for TAK1 in NF-κB activation differs depending on the stimuli, whereas TAK1 functions as an essential activator of Jnk in response to a variety of stimuli.

To further elucidate how TAK1 regulates BCR-mediated proliferative responses, we investigated BCR-induced gene expression profiles by microarray analysis. The BCR-mediated expression of genes involved in cell cycling and survival was not impaired in *Cd19*$^{Cre/+}$*Map3k7*$^{flox/-}$ B cells (**Supplementary Table 1** online). The upregulation of cyclin D2 protein as well as mRNA was comparable in BCR-stimulated control and TAK1-deficient B cells (**Supplementary Fig. 4** and **Supplementary Table 1** online). However, the downregulation of p27^{Kip1} expression was impaired in *Cd19*$^{Cre/+}$*Map3k7*$^{flox/-}$ B cells, suggesting that G1-S progression was impaired at the level of p27 expression (**Supplementary Fig. 4** online).

Bcl10 and CARD11 are crucial for BCR-induced Jnk and NF-κB activation. In contrast, MALT1 is required for the activation of NF-κB

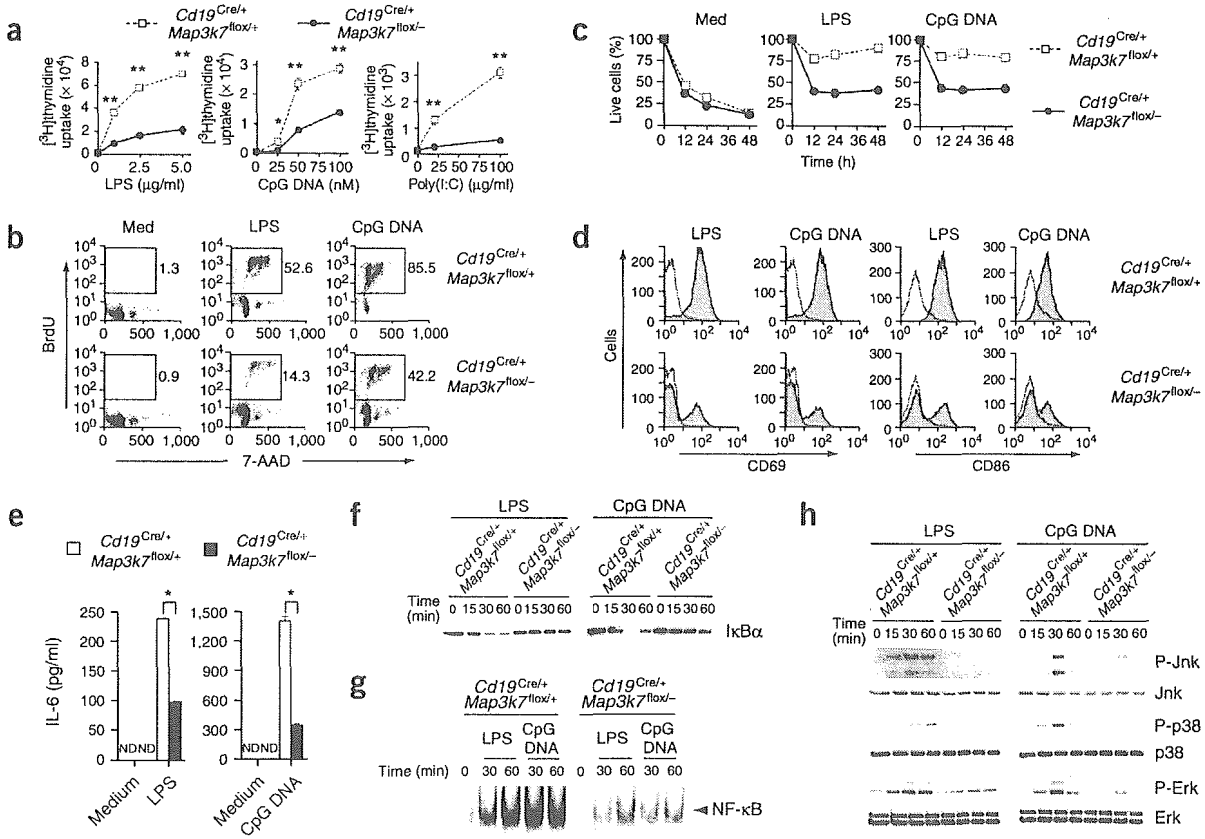

Figure 5 Impaired B cell activation in response to TLR ligands in *Cd19*$^{Cre/+}$*Map3k7*$^{flox/-}$ mice. (**a**) Proliferation of purified splenic B cells treated 48 h with various stimuli (horizontal axes), assessed by [^{3}H]thymidine incorporation. Data are mean ± s.d. of triplicate cultures. *, $P < 0.05$ and **, $P < 0.005$, versus TAK1-deficient cells (Student's *t*-test). (**b**) Cell cycle profiles of B cells left untreated (Med) or after *in vitro* stimulation with 5 μg/ml of LPS or 100 nM CpG DNA. Cells were labeled with BrdU and were analyzed by flow cytometry 24 h after stimulation. Numbers beside boxed areas indicate percentage of cells in S phase. (**c**) Defective survival of *Cd19*$^{Cre/+}$*Map3k7*$^{flox/-}$ cells. B cells were stimulated with 5 μg/ml of LPS or 100 nM CpG DNA. Viability of cells was assessed by staining with annexin V–indocarbocyanine followed by flow cytometry (time, horizontal axes). (**d**) Surface expression of activation markers. B cells were left unstimulated (open) or were stimulated for 24 h with 5 μg/ml of LPS or 100 nM CpG DNA (filled). Cells were then stained with anti-CD69 or anti-CD86. (**e**) ELISA of IL-6 production by B cells stimulated with LPS (20 μg/ml) or CpG DNA (2 μM). Data are mean ± s.d. of triplicate samples of one representative of three independent experiments. *, $P < 0.005$, versus TAK1-deficient cells (Student's *t*-test). (**f**) Immunoblot of IκBα degradation by B cells in response to LPS (20 μg/ml) or CpG DNA (2 μM). (**g**) EMSA of NF-κB DNA-binding activity in nuclear extracts of purified splenic B cells treated (time, above lanes) with LPS (20 μg/ml) or CpG DNA (2 μM). (**h**) Immunoblot of lysates of B cells stimulated (time, above lanes) with LPS (20 μg/ml) or CpG DNA (2 μM). Antibodies, right margin. All results are representative of three different experiments.

but not Jnk downstream of Bcl10 in BCR signaling. Mice lacking Bcl10, CARD11 or MALT1 are reported to have defects in the development of B-1 B cells and B cell activation. That prompted us to hypothesize that TAK1 may be recruited to the Bcl10 complex to activate Jnk. Therefore, we examined the association of TAK1 and Bcl10 using the human B cell line WEHI-231. When the cells were stimulated with antibody to IgM (anti-IgM), Bcl10 was immunoprecipitated together with TAK1 and with CARD11 (**Fig. 6i**). In contrast, TAK1 failed to precipitate together with Bcl10 in LPS-stimulated cells (**Fig. 6i**). These results suggest that TAK1 is recruited to the Bcl10 complex after BCR stimulation and is involved in Bcl10-mediated Jnk activation in B cells.

TAK1 is required for *in vivo* immune responses

We further investigated the involvement of TAK1 in humoral immune responses. The serum immunoglobulin concentrations of all isotypes except IgM were lower in *Cd19*$^{Cre/+}$*Map3k7*$^{flox/-}$ B cells than in *Cd19*$^{Cre/+}$*Map3k7*$^{flox/+}$ B cells (**Fig. 7a**). To induce humoral immune responses, we challenged *Cd19*$^{Cre/+}$*Map3k7*$^{flox/-}$ and littermate *Cd19*$^{Cre/+}$*Map3k7*$^{flox/+}$ mice with the T cell–dependent antigen nitrophenol conjugated to chicken γ-globulin or with the T cell–independent type II antigen trinitrophenol conjugated to Ficoll. The production of antigen-specific IgG1 in response to the T cell–dependent antigen was considerably impaired in *Cd19*$^{Cre/+}$*Map3k7*$^{flox/-}$ mice compared with that of control *Cd19*$^{Cre/+}$*Map3k7*$^{flox/+}$ mice, whereas IgM titers were similar in both groups of mice (**Fig. 7b**). Similarly, IgG3 production of *Cd19*$^{Cre/+}$*Map3k7*$^{flox/-}$ mice injected with trinitrophenol-Ficoll was impaired compared with that of control mice (**Fig. 7c**). This might have been due to the reduction in B-1 B cells in *Cd19*$^{Cre/+}$*Map3k7*$^{flox/-}$ mice, as B-1 B cells are the chief mediators of the T cell–independent response[24]. Impaired activation of B cells may also contribute to the defect in the istype switching. These results show that TAK1 is required for the appropriate induction of humoral immune responses.

DISCUSSION

Here we generated TAK1-deficient mice and a mouse strain with conditional expression of a *Map3k7* allele. *In vitro* studies have

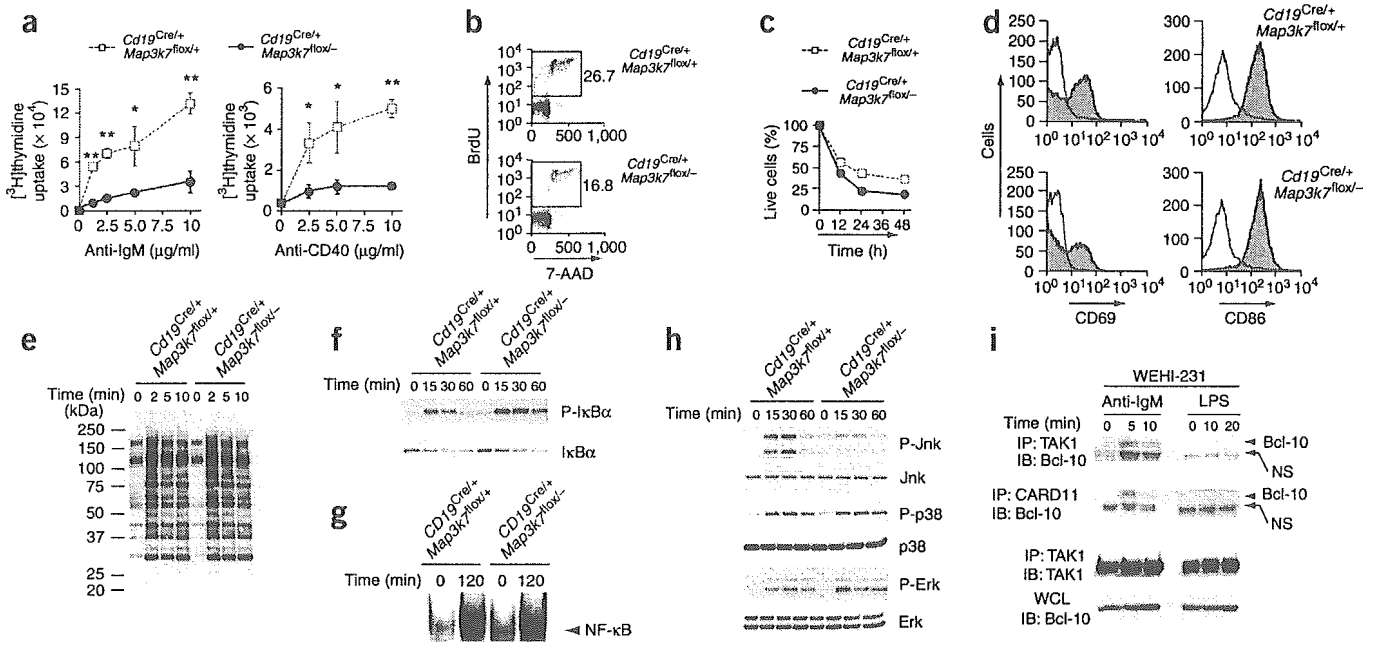

Figure 6 Impaired B cell activation by crosslinking of BCRs in *Cd19*$^{Cre/+}$*Map3k7*$^{flox/-}$ mice. **(a)** Proliferation of purified splenic B cells stimulated for 48 h (stimuli, horizontal axes), assessed by [^{3}H]thymidine incorporation. Data are mean ± s.d. of triplicate cultures. *, $P < 0.05$ and **, $P < 0.005$, versus TAK1-deficient cells (Student's *t*-test). **(b)** Cell cycle profiles of B cells stimulated with 5 μg/ml of anti-IgM. Cells were labeled with BrdU and were analyzed by flow cytometry 24 h after stimulation. Numbers beside boxed areas indicate percentages of cells in S phase. **(c)** Viability of B cells stimulated with 5 μg/ml of anti-IgM, assessed by staining with annexin V–indocarbocyanine followed by flow cytometry (time, horizontal axis). **(d)** Flow cytometry of purified splenic B cells left unstimulated (open) or stimulated for 24 h with 5 μg/ml of anti-IgM (filled) and then stained with anti-CD69 or anti-CD86. **(e)** Total tyrosine phosphorylation of B cells stimulated with 20 μg/ml of anti-IgM (time, above lanes). **(f)** Immunoblot of IκBα degradation in B cells in response to 20 μg/ml of anti-IgM. **(g)** EMSA of NF-κB DNA-binding activity in nuclear extracts from purified splenic B cells stimulated for 2 h with 20 μg/ml of anti-IgM. **(h)** MAPK activation in BCR-stimulated B cells stimulated with 20 μg/ml of anti-IgM (time, above lanes). **(i)** Association between TAK1 and Bcl10. WEHI-231 cells (1.5 × 10^8) were stimulated with 20 μg/ml of anti-IgM or 20 μg/ml of LPS (time, above lanes); cell lysates were immunoprecipitated (IP) with anti-TAK1 or anti-CARD11 and immunoprecipitates or whole-cell lysates (WCL) were analyzed by immunoblot (IB; antibodies, left margin). All results are representative of three different experiments. NS, nonspecific band.

suggested that TAK1 has an important function in IL-1R and TNFR signaling by forming a complex with TAB1 and TAB2 (refs. 11,14,15). However, mice lacking TAB2 have normal IL-1β responses[18]. The function of TAB1 in the IL-1R signaling is still unclear, although involvement TAB1 in TGF-β signaling has been reported in studies of TAB1-deficient mice[19]. It is possible TAB3, a homolog of TAB2, functions redundantly in TAB2-deficient mice[16,17,25,26]. In contrast, TAK1-deficient MEFs showed considerably impaired responses, including activation of NF-κB and MAPKs in response to IL-1β stimulation. However, IL-1β-induced production of IL-6 or activation of NF-κB was not completely abrogated in TAK1-deficient MEFs, indicating IL-1R activates both TAK1-dependent and TAK1-independent signaling pathways.

The involvement of TAK1 in TNFR signaling is controversial. Initially, TAK1 was reported to bind TRAF6 but not TRAF2, an important mediator of TNFR signaling[8]. However, other *in vitro* studies have shown that TAK1 regulates TNF-induced NF-κB activation[11,26]. Our results have demonstrated that TAK1 is critical for activation of both NF-κB and MAPKs in response to TNF. In addition, stimulation with TNF alone induced massive cell death in *Map3k7*$^{-/-}$ MEFs. In wild-type cells, TNF stimulation activates NF-κB and MAPK pathways, which mediate cell survival and proliferation by expressing target genes such as those encoding inhibitor of apoptosis and Bcl-2 family members[1]. TNF simultaneously activates the apoptotic pathway by recruiting Fas-associated death domain and caspase 8, followed by activation of caspase 3. This pathway does not require protein synthesis[1]. It is believed that the balance between life and death signals determines the fate of the cell. TNF kills wild-type cells when protein synthesis is inhibited. Given that TNF-induced NF-κB and MAPK activation was considerably impaired in *Map3k7*$^{-/-}$ MEFs, cells lacking TAK1 might fail to induce survival genes that protect cells from TNF-induced cell death.

The function of TAK1 in TLR signaling is less well understood. As B cells express various TLRs and are activated in response to pathogen-associated molecular patterns, we examined the involvement of TAK1 in TLR signaling using the B cell system as a model. Although most TLRs as well as IL-1R share MyD88 as an adaptor for triggering intracellular signaling, several other adaptor molecules such as TRIF contribute to the TLR signaling pathways[3]. Responses to TLR3, TLR4 and TLR9 ligands were considerably impaired in TAK1-defeicient B cells. Moreover, activation of MAPKs and NF-κB in response to TLR4 and TLR9 ligand was consistently impaired, although the activation was not completely abrogated even in the absence of TAK1. As TLR9 signaling depends completely on MyD88, it is obvious that TAK1 is important for MyD88-dependent signaling pathways. TLR4 activates MyD88-dependent and TRIF-dependent pathways. Both signaling pathways can activate NF-κB and MAPKs, although the time course differs. The MyD88-dependent pathway governs early activation of these signaling molecules, whereas the TRIF-dependent pathway is responsible for sustaining the activation[27,28]. In B cells, both MyD88 and TRIF are required for TLR4-induced proliferative response. In TLR4 signaling, the activation of NF-κB and MAPKs was considerably

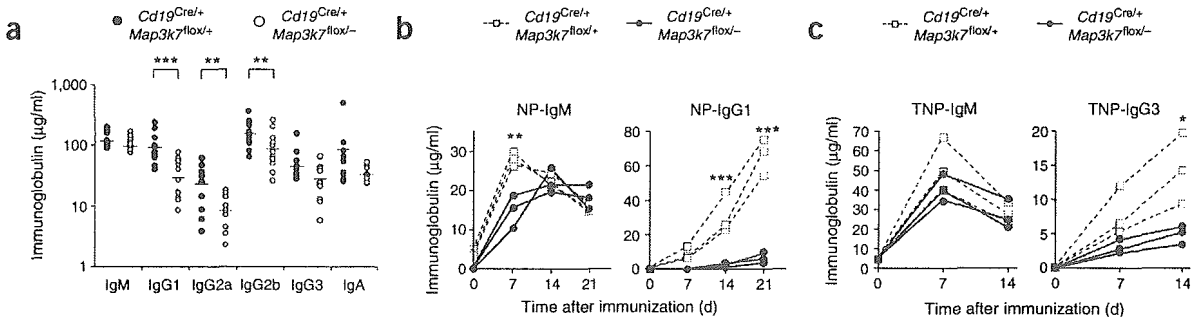

Figure 7 Impaired immune responses in *Cd19*$^{Cre/+}$*Map3k7*$^{flox/-}$ mice. (**a**) Reduced basal immunoglobulin titers in *Cd19*$^{Cre/+}$*Map3k7*$^{flox/-}$ mice. Immunoglobulin isotypes were measured by ELISA in the sera of nonimmunized 8-week-old *Cd19*$^{Cre/+}$*Map3k7*$^{flox/+}$ mice ($n = 12$) or *Cd19*$^{Cre/+}$*Map3k7*$^{flox/-}$ mice ($n = 12$). Results are from individual mice. (**b**) Impaired T cell–dependent antibody responses in *Cd19*$^{Cre/+}$*Map3k7*$^{flox/-}$ mice. Mice were immunized with nitrophenol–chicken γ-globulin, and nitrophenol (NP)–specific IgM and IgG1 production was measured by ELISA 7, 14 and 21 d after immunization. Results are from three (of five) representative mice per genotype. (**c**) Impaired T cell–independent type II antibody responses in *Cd19*$^{Cre/+}$*Map3k7*$^{flox/-}$ mice. Mice were immunized with trinitrophenol-Ficoll, and trinitrophenol (TNP)–specific IgM and IgG3 production was measured 7 and 14 d after immunization. Results are from three (of five) representative mice per genotype. *, $P < 0.05$; **, $P < 0.01$ and ***, $P < 0.005$, versus TAK1-deficient cells (Student's *t*-test).

impaired in TAK1-deficient B cells at all time points examined, suggesting that MyD88-dependent and TRIF-dependent activation of these molecules depends entirely on TAK1.

Notably, TAK1 is also critical for B cell proliferation as well as Jnk activation in response to BCR crosslinking. Nevertheless, the activation of NF-κB and induction of NF-κB target genes induced by BCR-crosslinking was not impaired in TAK1-deficient B cells. In BCR signaling, a complex of CARD11, Bcl10 and MALT1 transduces signals to NF-κB and MAPKs downstream of protein kinase C-β[22]. CARD11 recruits Bcl10 to lipid rafts after stimulation. Bcl10 targets NF-κB essential modulator for K63-linked polyubiquitination through Ubc13 and MALT1 and activates NF-κB[29]. B cells from *Card11*$^{-/-}$, *Bcl10*$^{-/-}$ or *Malt1*$^{-/-}$ mice are reported to have defects in BCR signaling[30–36]. CARD11 is required for the activation of both NF-κB and Jnk[32]. Furthermore, *Bcl10*$^{-/-}$ B cells fail to activate NF-κB in response to BCR crosslinking. In contrast, B cells deficient in MALT1 (paracaspase) show impaired activation of NF-κB but not Jnk[34], indicating that Jnk is activated in a CARD11- and Bcl10-dependent, MALT1-independent signaling pathway. Given that TAK1 phosphorylates IKKs and MKK6 in IL-1β signaling, it is plausible that TAK1 is activated downstream of the CARD11-Bcl10-MALT1 complex and phosphorylates MAPKKs. In fact, we found that TAK1 interacted with Bcl10 in response to BCR crosslinking, indicating that TAK1 is recruited to the Bcl10 complex after BCR stimulation to induce Jnk activation. Although published work has shown that RNA interference–mediated knockdown of TAK1 in Jurkat cells results in diminished NF-κB activation in TCR signaling[23], our study has demonstrated that TAK1 is dispensable for NF-κB activation, at least in BCR signaling. That earlier report also showed that TRAF6 functions downstream of Bcl10 and MALT1 to activate NF-κB in TCR signaling[23]. Given that TAK1 interacts with Bcl10 in response to BCR but not LPS stimulation, it is likely that TAK1 is activated by Bcl10 without the intervention of TRAF6 in BCR signaling. As TAK1 is required for the activation of Jnk but not NF-κB, MALT1-mediated activation of the IKK complex probably occurs independently of TAK1. These results collectively indicate that in B cells, CARD11 and Bcl10 might activate TAK1 and MALT1 to regulate MAPKKs and IKKs, respectively.

Although TAK1-deficient B cells failed to proliferate in response to BCR crosslinking, activation of NF-κB was not impaired. Consistent with that finding, the upregulation of cyclin D2 was not altered in TAK1-deficient B cells. However, downregulation of p27^{Kip1} was impaired in TAK1-deficient B cells, suggesting that TAK1-dependent signaling might regulate G1-S progression at the level of p27^{Kip1} degradation. So far, it is not clear whether Jnk alone is responsible for the defect in the proliferation in TAK1-deficient B cells. It is possible that TAK1 regulates the activation of as-yet-unknown signaling pathway(s) in addition to Jnk and that the pathways cooperatively control BCR-mediated proliferation. Additional studies are needed to clarify the molecular mechanisms of cell cycle progression in BCR signaling.

Involvement of TAK1 in early embryogenesis modifying bone morphogenic protein signaling has been suggested[37]. *Map3k7*$^{-/-}$ embryos died at E9.5–E10.5. Mice deficient in genes encoding molecules involved in NF-κB signaling, such as RelA (also called p65) and IKKβ, die *in utero* due to massive liver apoptosis[38–41]. However, *Map3k7*$^{-/-}$ mice die before the initiation of fetal liver development, suggesting that the function of TAK1 in embryonic development is not explained by NF-κB inhibition. TAB1-deficient mice die between E15.5 and E18.5 due to edema and hemorrhage, and TAB2-deficient mice die between E11.5 and E12.5 due to liver apoptosis[18,19]. Thus, the function of TAK1 in embryogenesis might be independent of TAB1 or TAB2. The TAK1-NLK-STAT3 cascade is essential for TGF-β-mediated mesoderm formation in xenopus embryos[42]. Additional studies will be needed to clarify the mechanisms of the involvement of TAK1 in early embryogenesis.

In conclusion, we have shown here that TAK1 is essential for MAPK and NF-κB activation in response to TLR, IL-1R and TNFR stimulation. Consistent with those findings, TAK1-deficient cells failed to activate in response to TLR ligands, IL-1β and TNF. Antigen-induced B cell proliferation as well as immune responses to experimental antigens were considerably impaired in mice with B cell–specific TAK1-deficiency, indicating that TAK1 is involved in both innate and adaptive immunity. These data provide genetic evidence that TAK1 kinase has nonredundant functions in signaling pathways in inflammatory and immune responses.

METHODS

Generation of *Map3k7* mutant mice. Phage clones containing mouse *Map3k7* were isolated by screening of a 129/SvJ genomic library (Stratagene) with a probe corresponding to the 5′ end of mouse TAK1 cDNA. A targeting vector was designed to flank exon 2, containing the sequence encoding the ATP-binding site, with two *lox*P sites. The floxed neomycin-resistance gene fragment was inserted into intron 1 of *Map3k7*. A 1.0–kilobase (kb) *Cla*I–*Bam*HI

fragment was used as the 5′ homology region; a 2.5-kb *Xba*I–*Sal*I fragment, which contains exon 2 of *Map3k7*, was inserted between the two *lox*P sites; and a 6.0-kb *Not*I–*Sac*II fragment was used as the 3′ homology region. The herpes simplex virus thymidine kinase gene was used for negative selection of clones with random integration. A total of 30 μg of *Sac*II-linearized vector was electroporated into E14.1 embryonic stem cells. After positive and negative selection with G418 and ganciclovir, drug-resistant clones were picked up and were screened by PCR and Southern blot analysis. These clones were individually microinjected into blastocysts derived from C57BL/6 mice and were transferred to pseudopregnant females. Matings of chimeric male mice to C57BL/6 female mice resulted in transmission of the floxed allele to the germline. *Map3k7*$^{flox/+}$ or *Map3k7*$^{flox/flox}$ mice were bred with transgenic mouse line carrying the *Cre* transgene under control of the cytomegalovirus immediate early enhancer–chicken β-actin hybrid (*CAG*) promoter[43] to generate the *CAG*$^{Cre/+}$*Map3k7*$^{flox/+}$ (genotype, *Map3k7*$^{+/-}$), which were then intercrossed to generate *CAG*$^{Cre/+}$*Map3k7*$^{flox/flox}$ (genotype, *Map3k7*$^{-/-}$) mice. All animal experiments were done with the approval of the Animal Research Committee of the Research Institute for Microbial Diseases (Osaka University, Osaka, Japan).

Establishment of *Map3k7*$^{-/-}$ MEFs. MEFs were obtained from E13.5 *Map3k7*$^{flox/flox}$ embryos, were immortalized according to a general 3T3 protocol[44] and were cloned. For excision of the floxed genomic fragment containing exon 2, two different clones of *Map3k7*$^{flox/flox}$ MEFs were infected with retrovirus expressing Cre protein together with GFP or were infected with GFP alone (to establish control MEFs). GFP$^+$ cells were sorted by FACSVantage (Becton Dickinson) and then were analyzed by Southern blot and immunoblot to confirm genotype.

Generation of mice with B cell–specific TAK1 deficiency. Mice carrying the *Cre* transgene under control of the *Cd19* promoter[45] were bred with *Map3k7*$^{+/-}$ mice to generate *Cd19*$^{Cre/+}$*Map3k7*$^{+/-}$ mice. These mice were mated with *Map3k7*$^{flox/flox}$ mice; *Cd19*$^{Cre/+}$*Map3k7*$^{flox/+}$ or *Cd19*$^{Cre/+}$*Map3k7*$^{flox/-}$ offspring were used for analysis.

Purification of B cells. Resting B cells were isolated from single-cell suspensions of spleen cells by depletion of CD43$^+$ cells with anti-CD43 magnetic beads (MACS; Miltenyi Biotec). Cell purity was typically more than 95% B220$^+$, as assessed by flow cytometry.

Immunoblot analysis. Cells were lysed in a lysis buffer containing 1.0% Nonidet-P40, 150 mM NaCl, 20 mM Tris-HCl, pH 7.5, 1 mM EDTA and a protease inhibitor 'cocktail' (Roche). Lysates were separated by SDS-PAGE and were transferred onto polyvinylidene difluoride membranes (BioRad). After membranes were blotted with antibodies, proteins on membranes were visualized with an enhanced chemiluminescence system (Perkin-Elmer). Polyclonal anti-TAK1, anti-TAB1, anti-TAB2 and anti-IRAK-1 were as described[8,15,46]. Polyclonal antibody to phosphorylated Jnk (anti-phospho-Jnk), anti-phospho-p38, anti-phospho-Erk and anti-phospho-IκBα were purchased from Cell Signaling. Polyclonal anti-Jnk, anti-p38, anti-Erk, anti-IκBα, anti-p27^{Kip1} and anti–cyclin D2 and monoclonal anti-Bcl10 (clone 331.3) were from Santa Cruz. Monoclonal anti-phosphotyrosine (clone 4G10) was purchased from Upstate Biotechnology. Polyclonal anti-CARD11 was from Alexis Biochemicals.

Luciferase reporter assay. HEK293 cells were transiently transfected with 100 ng of either NF-κB (5×) or AP-1 luciferase reporter plasmids, together with a total of 1.0 μg expression vector(s). Then, 48 h later, the luciferase activity in the total cell lysate was measured with the Dual-luciferase reporter assay system (Promega).

Measurement of IL-6 production. MEFs (2×10^4) and purified splenic B cells (5×10^4) were stimulated for 48 h with recombinant mouse IL-1β (R&D Systems) and LPS (Sigma) or with CpG DNA (ODN1668; Hokkaido System Science), respectively. Culture supernatants were collected and IL-6 was measured with an ELISA kit (R&D Systems).

Cell viability. MEFs (2×10^5) were seeded onto six-well plates and were treated for 24 h with various concentrations of recombinant mouse TNF (R&D Systems). Purified splenic B cells (1×10^6) were stimulated with LPS, CpG DNA or anti-IgM (Jackson ImmunoResearch) for various periods. Cell viability was assessed with annexin V–indocarbocyanine (BioVision) and a FACSCalibur (Becton Dickinson).

Electrophoretic mobility-shift assay (EMSA). MEFs (1×10^6) or purified splenic B cells (5×10^6) were treated with stimuli for various periods. Nuclear extracts were purified from cells, were incubated with a probe specific for the NF-κB DNA-binding site, were separated by electrophoresis and were visualized by autoradiography as described[47].

Flow cytometry. Single-cell suspensions were prepared from thymi, bone marrow, spleens and peritoneal cavities of untreated mice. Cells were stained with fluorescein isothiocyanate–, phycoerythrin- or allophycocyanin-conjugated antibodies (Pharmingen) and then were analyzed on a FACSCalibur.

***In vivo* immunization and ELISA.** Mice were immunized intraperitoneally with 50 μg nitrophenol–chicken γ-globulin (Biosearch Technologies) precipitated with Imject alum (Pierce) or with 25 μg trinitrophenol-Ficoll (Biosearch Technologies). Antigen- and isotype-specific antibodies were measured by ELISA in sera collected from peripheral blood at various time points, on plates coated with nitrophenol-BSA or trinitrophenol-BSA. Antibodies to mouse IgM, IgG1, IgG2a, IgG2b, IgG3 and IgA were purchased from Southern Biotechnology.

B cell proliferation assay. Purified splenic B cells (5×10^4) were cultured in 96-well plates for 48 h with various concentrations of LPS, CpG DNA, poly(I:C) (Amersham), anti-IgM or anti-CD40 (Pharmingen). Samples were pulsed with 1 μCi [^{3}H]thymidine for the last 12 h and then ^{3}H uptake was measured with a β-scintillation counter (Packard).

Cell cycle analysis. Cell cycles of B cells were analyzed with the BrdU Flow Kit (Pharmingen) according to the manufacturer's instructions. Cells were cultured with LPS, CpG DNA or anti-IgM for 24 h, were pulsed with 10 μM BrdU for an additional 16 h, were stained with fluorescein isothiocyanate–anti-BrdU and 7-amino-actinomycin D and then were analyzed by flow cytometry.

Microarray analysis. Purified splenic B cells were treated for 4 h with or without anti-IgM (20 μg/ml). Total RNA was extracted with an RNeasy kit (Qiagen), and double-stranded DNA was synthesized from 10 μg of total RNA with the SuperScript Choice System (Invitrogen) primed with a T7-Oligo primer (Affymetrix). This cDNA was used to prepare biotin-labeled cRNA by an *in vitro* transcription reaction done with T7 RNA polymerase in the presence of biotinylated ribonucleotides, according to the manufacturer's protocol (Enzo Diagnostics). The cRNA product was purified with an RNeasy kit and fragmented and was hybridized to Affymetrix mouse expression array A430.2 microarray chips according to the manufacturer's protocol (Affymetrix). The hybridized chips were stained and washed and were scanned with a GeneArray Scanner (Affymetrix).

Accession code. GEO: microarray data, GSE3065.

Note: Supplementary information is available on the Nature Immunology website.

ACKNOWLEDGMENTS

We thank R.C. Rickert (The Burnham Institute, La Jolla, California) for providing *Cd19-Cre* mice; J. Miyazaki (Osaka University, Suita, Japan) for providing *CAG-Cre* mice; T. Kitamura (University of Tokyo, Tokyo, Japan) for providing retrovirus vector; D.T. Golenbock (University of Massachusetts Medical School, Worcester, Massachusetts) for providing NF-κB reporter; T. Kaisho and Y. Kumagai for discussions; K. Nakamura for cell sorting; A. Shibano, M. Shiokawa, Y. Fujiwara and N. Kitagaki for technical assistance; and M. Hashimoto and E. Horita for secretarial assistance. Supported by Special Coordination Funds, the Ministry of Education, Culture, Sports, Science and Technology.

COMPETING INTERESTS STATEMENT

The authors declare that they have no competing financial interests.

Published online at http://www.nature.com/natureimmunology/
Reprints and permissions information is available online at http://npg.nature.com/reprintsandpermissions/

1. Aggarwal, B.B. Signalling pathways of the TNF superfamily: a double-edged sword. *Nat. Rev. Immunol.* **3**, 745–756 (2003).

2. Dinarello, C.A. Biologic basis for interleukin-1 in disease. *Blood* **87**, 2095–2147 (1996).
3. Akira, S. & Takeda, K. Toll-like receptor signalling. *Nat. Rev. Immunol.* **4**, 499–511 (2004).
4. Baud, V. & Karin, M. Signal transduction by tumor necrosis factor and its relatives. *Trends Cell Biol.* **11**, 372–377 (2001).
5. Deng, L. *et al.* Activation of the IκB kinase complex by TRAF6 requires a dimeric ubiquitin-conjugating enzyme complex and a unique polyubiquitin chain. *Cell* **103**, 351–361 (2000).
6. Wang, C. *et al.* TAK1 is a ubiquitin-dependent kinase of MKK and IKK. *Nature* **412**, 346–351 (2001).
7. Ghosh, S. & Karin, M. Missing pieces in the NF-κB puzzle. *Cell* **109**, S81–S96 (2002).
8. Ninomiya-Tsuji, J. *et al.* The kinase TAK1 can activate the NIK-IκB as well as the MAP kinase cascade in the IL-1 signalling pathway. *Nature* **398**, 252–256 (1999).
9. Yamaguchi, K. *et al.* Identification of a member of the MAPKKK family as a potential mediator of TGF-β signal transduction. *Science* **270**, 2008–2011 (1995).
10. Vidal, S. *et al.* Mutations in the *Drosophila* dTAK1 gene reveal a conserved function for MAPKKKs in the control of rel/NF-κB-dependent innate immune responses. *Genes Dev.* **15**, 1900–1912 (2001).
11. Takaesu, G. *et al.* TAK1 is critical for IκB kinase-mediated activation of the NF-κB pathway. *J. Mol. Biol.* **326**, 105–115 (2003).
12. Irie, T., Muta, T. & Takeshige, K. TAK1 mediates an activation signal from toll-like receptor(s) to nuclear factor-κB in lipopolysaccharide-stimulated macrophages. *FEBS Lett.* **467**, 160–164 (2000).
13. Wan, J. *et al.* Elucidation of the c-Jun N-terminal kinase pathway mediated by Estein-Barr virus-encoded latent membrane protein 1. *Mol. Cell. Biol.* **24**, 192–199 (2004).
14. Shibuya, H. *et al.* TAB1: an activator of the TAK1 MAPKKK in TGF-β signal transduction. *Science* **272**, 1179–1182 (1996).
15. Takaesu, G. *et al.* TAB2, a novel adaptor protein, mediates activation of TAK1 MAPKKK by linking TAK1 to TRAF6 in the IL-1 signal transduction pathway. *Mol. Cell* **5**, 649–658 (2000).
16. Ishitani, T. *et al.* Role of the TAB2-related protein TAB3 in IL-1 and TNF signaling. *EMBO J.* **22**, 6277–6288 (2003).
17. Cheung, P.C., Nebreda, A.R. & Cohen, P. TAB3, a new binding partner of the protein kinase TAK1. *Biochem. J.* **378**, 27–34 (2004).
18. Sanjo, H. *et al.* TAB2 is essential for prevention of apoptosis in fetal liver but not for interleukin-1 signaling. *Mol. Cell. Biol.* **23**, 1231–1238 (2003).
19. Komatsu, Y. *et al.* Targeted disruption of the Tab1 gene causes embryonic lethality and defects in cardiovascular and lung morphogenesis. *Mech. Dev.* **119**, 239–249 (2002).
20. Wagner, M. *et al.* IL-12p70-dependent Th1 induction by human B cells requires combined activation with CD40 ligand and CpG DNA. *J. Immunol.* **172**, 954–963 (2004).
21. Kurosaki, T. Regulation of B-cell signal transduction by adaptor proteins. *Nat. Rev. Immunol.* **2**, 354–363 (2002).
22. Thome, M. CARMA1, BCL-10 and MALT1 in lymphocyte development and activation. *Nat. Rev. Immunol.* **4**, 348–359 (2004).
23. Sun, L., Deng, L., Ea, C.K., Xia, Z.P. & Chen, Z.J. The TRAF6 ubiquitin ligase and TAK1 kinase mediate IKK activation by BCL10 and MALT1 in T lymphocytes. *Mol. Cell* **14**, 289–301 (2004).
24. Sidorova, E.V., Li-Sheng, L., Devlin, B., Chernishova, I. & Gavrilova, M. Role of different B-cell subsets in the specific and polyclonal immune response to T-independent antigens type 2. *Immunol. Lett.* **88**, 37–42 (2003).
25. Jin, G. *et al.* Identification of a human NF-κB-activating protein, TAB3. *Proc. Natl. Acad. Sci. USA* **101**, 2028–2033 (2004).
26. Kanayama, A. *et al.* TAB2 and TAB3 activate the NF-κB pathway through binding to polyubiquitin chains. *Mol. Cell* **15**, 535–548 (2004).
27. Kawai, T., Adachi, O., Ogawa, T., Takeda, K. & Akira, S. Unresponsiveness of MyD88-deficient mice to endotoxin. *Immunity* **11**, 115–122 (1999).
28. Yamamoto, M. *et al.* Role of adaptor TRIF in the MyD88-independent toll-like receptor signaling pathway. *Science* **301**, 640–643 (2003).
29. Zhou, H. *et al.* Bcl10 activates the NF-κB pathway through ubiquitination of NEMO. *Nature* **427**, 167–171 (2004).
30. Ruland, J. *et al.* Bcl10 is a positive regulator of antigen receptor-induced activation of NF-κB and neural tube closure. *Cell* **104**, 33–42 (2001).
31. Egawa, T. *et al.* Requirement for CARMA1 in antigen receptor-induced NF-κB activation and lymphocyte proliferation. *Curr. Biol.* **13**, 1252–1258 (2003).
32. Hara, H. *et al.* The MAGUK family protein CARD11 is essential for lymphocyte activation. *Immunity* **18**, 763–775 (2003).
33. Newton, K. & Dixit, V.M. Mice lacking the CARD of CARMA1 exhibit defective B lymphocyte development and impaired proliferation of their B and T lymphocytes. *Curr. Biol.* **13**, 1247–1251 (2003).
34. Ruefli-Brasse, A.A., French, D.M. & Dixit, V.M. Regulation of NF-κB-dependent lymphocyte activation and development by paracaspase. *Science* **302**, 1581–1584 (2003).
35. Ruland, J., Duncan, G.S., Wakeham, A. & Mak, T.W. Differential requirement for Malt1 in T and B cell antigen receptor signaling. *Immunity* **19**, 749–758 (2003).
36. Xue, L. *et al.* Defective development and function of Bcl10-deficient follicular, marginal zone and B1 B cells. *Nat. Immunol.* **4**, 857–865 (2003).
37. Munoz-Sanjuan, I., Bell, E., Altmann, C.R., Vonica, A. & Brivanlou, A.H. Gene profiling during neural induction in *Xenopus laevis*: regulation of BMP signaling by post-transcriptional mechanisms and TAB3, a novel TAK1-binding protein. *Development* **129**, 5529–5540 (2002).
38. Beg, A.A., Sha, W.C., Bronson, R.T., Ghosh, S. & Baltimore, D. Embryonic lethality and liver degeneration in mice lacking the RelA component of NF-κB. *Nature* **376**, 167–170 (1995).
39. Tanaka, M. *et al.* Embryonic lethality, liver degeneration, and impaired NF-κB activation in IKK-β-deficient mice. *Immunity* **10**, 421–429 (1999).
40. Li, Q., Van Antwerp, D., Mercurio, F., Lee, K.F. & Verma, I.M. Severe liver degeneration in mice lacking the IκB kinase 2 gene. *Science* **284**, 321–325 (1999).
41. Rudolph, D. *et al.* Severe liver degeneration and lack of NF-κB activation in NEMO/IKKγ-deficient mice. *Genes Dev.* **14**, 854–862 (2000).
42. Ohkawara, B. *et al.* Role of the TAK1-NLK-STAT3 pathway in TGF-β-mediated mesoderm induction. *Genes Dev.* **18**, 381–386 (2004).
43. Sakai, K., Mitani, K. & Miyazaki, J. Efficient regulation of gene expression by adenovirus vector-mediated delivery of the CRE recombinase. *Biochem. Biophys. Res. Commun.* **217**, 393–401 (1995).
44. Todaro, G.J. & Green, H. Quantitative studies of the growth of mouse embryo cells in culture and their development into established lines. *J. Cell Biol.* **17**, 299–313 (1963).
45. Rickert, R.C., Roes, J. & Rajewsky, K. B lymphocyte-specific, Cre-mediated mutagenesis in mice. *Nucleic Acids Res.* **25**, 1317–1318 (1997).
46. Sato, S. *et al.* A variety of microbial components induce tolerance to lipopolysaccharide by differentially affecting MyD88-dependent and -independent pathways. *Int. Immunol.* **14**, 783–791 (2002).
47. Sato, S. *et al.* Synergy and cross-tolerance between toll-like receptor (TLR) 2- and TLR4-mediated signaling pathways. *J. Immunol.* **165**, 7096–7101 (2000).

Immunity, Vol. 22, 305–316, March, 2005, Copyright ©2005 by Elsevier Inc. DOI 10.1016/j.immuni.2005.01.014

Nonredundant Roles of Sema4A in the Immune System: Defective T Cell Priming and Th1/Th2 Regulation in Sema4A-Deficient Mice

Atsushi Kumanogoh,[1,10] Takashi Shikina,[1,7,10] Kazuhiro Suzuki,[1] Satoshi Uematsu,[2] Kazunori Yukawa,[4] Shin-Ichiro Kashiwamura,[5] Hiroko Tsutsui,[6] Midori Yamamoto,[1] Hyota Takamatsu,[1] Elizabeth P. Ko-Mitamura,[1] Noriko Takegahara,[1] Satoko Marukawa,[1] Isao Ishida,[1] Hiroshi Morishita,[1] Durbaka V.R. Prasad,[1] Manabu Tamura,[7] Masayuki Mizui,[1,8] Toshihiko Toyofuku,[1,8] Shizuo Akira,[2] Kiyoshi Takeda,[2,9] Masaru Okabe,[3] and Hitoshi Kikutani[1,*]

[1]Department of Molecular Immunology and CREST Program of JST
[2]Department of Host Defense and ERATO Program of JST
Research Institute for Microbial Diseases
[3]Genome Information Research Center
Osaka University
3-1 Yamada-oka
Suita
Osaka 565-0871
Japan
[4]Department of Physiology II
Wakayama Medical College
811-1 Kimiidera
Wakayama
Wakayama 641-0012
Japan
[5]Department of Immunology and Medical Zoology
[6]Laboratory of Host Defenses
Institute for Advanced Medical Sciences
Hyogo College of Medicine
Nishinomiya, 663-8501
Japan
[7]Department of Otolaryngology and Sensory Organ Surgery (E8)
[8]Department of Internal Medicine and Therapeutics
Osaka University Graduate School of Medicine
2-2 Yamada-oka
Suita
Osaka 565-0871
Japan
[9]Devision of Embryonic and Genetic Engineering
Medical Institute for Bioregulation
Kyushu University
3-1-1 Maidashi
Higashi-ku
Fukuoka 812-8582
Japan

Summary

The class IV semaphorin Sema4A provides a costimulatory signal to T cells. To investigate the possible developmental and regulatory roles of Sema4A in vivo, we generated Sema4A-deficient mice. Although Sema4A-deficient mice develop normally, DCs and T cells from knockout mice display poor allostimulatory activities and T helper cell (Th) differentiation, respectively. Interestingly, in addition to its expression on DCs, Sema4A is upregulated on Th1-differentiating cells, and it is necessary for in vitro Th1 differentiation and T-bet expression. Consequently, in vivo antigen-specific T cell priming and antibody responses against T cell-dependent antigens are impaired in the mutant mice. Additionally, Sema4A-deficient mice exhibit defective Th1 responses. Furthermore, reconstitution studies with antigen-pulsed DCs reveal that DC-derived Sema4A is important for T cell priming, while T cell-derived Sema4A is involved in developing Th1 responses. Collectively, these results indicate a nonredundant role of Sema4A not only in T cell priming, but also in the regulation of Th1/Th2 responses.

Introduction

Sema4A is a transmembrane protein belonging to the semaphorin family, several members of which have been identified as axonal guidance factors active during neuronal development (Kolodkin et al., 1993; Tamagnone and Comoglio, 2000; Pasterkamp and Kolodkin, 2003). *Sema4A* was identified originally as a semaphorin expressed in developing embryos, and Sema4A transcript levels increase gradually throughout embryonic development (Puschel et al., 1995), although its role in development is not yet known. In addition to its expression during embryogenesis, Sema4A is expressed in the brain, lung, kidney, testis, and spleen of adults (Kumanogoh et al., 2002a; Kikutani and Kumanogoh, 2003). In the immune system, Sema4A is preferentially expressed by bone marrow-derived and splenic dendritic cells (DCs) (Kumanogoh et al., 2002a). Expression of Sema4A also becomes detectable on the cell surface of T cells following activation (Kumanogoh et al., 2002a), although its precise expression profile and functional significance remain unclear.

A possible role for Sema4A in the immune response was suggested by studies with soluble Sema4A proteins and anti-Sema4A monoclonal antibody (mAb) (Kumanogoh et al., 2002a). Sema4A provides a costimulatory signal to T cells, that is, the addition of recombinant soluble Sema4A proteins enhances T cell proliferation and IL-2 production following stimulation with anti-CD3 mAb. Additionally, soluble Sema4A protein enhanced the mixed lymphocyte reactions (MLR) between allogeneic T cells and DCs, while an anti-Sema4A mAb blocked the MLR, suggesting that Sema4A plays a role in T cell activation by influencing the stimulatory interactions between T cells and DCs. The administration of soluble Sema4A proteins enhanced the in vivo generation of antigen-specific T cells. In contrast, administration of anti-Sema4A mAb blocked antigen-specific T cell priming. Furthermore, treatment of mice with anti-

*Correspondence: kikutani@ragtime.biken.osaka-u.ac.jp
[10]These authors contributed equally to this work.

Sema4A mAb inhibited the development of experimental autoimmune encephalomyelitis (EAE) induced by administration of a myelin oligodendrocyte glycoprotein (MOG)-derived peptide, due to the impaired generation of MOG-specific T cells (Kumanogoh et al., 2002a). However, the role of Sema4A in physiological and pathological immune responses remains to be determined.

Sema4A binding partners have been identified on the surface of activated T cells. Expression cloning revealed that Tim-2, a member of the T cell, immunoglobulin, and mucin domain proteins (Tim) family, is a receptor for Sema4A (Kumanogoh et al., 2002a). McIntire et al. (2001) identified a locus conferring susceptibility to mouse allergen-induced airway hypersensitivity, which they dubbed T cell and airway phenotype regulator (*Tapr*), and a new family of genes, designated *Tims* in this locus. Sequence polymorphisms within both mouse and human *Tim-1* have been suggested to contribute to the etiology of both mouse and human T helper cell (Th)2-dependent diseases such as asthma (McIntire et al., 2001; Kuchroo et al., 2003; Chae et al., 2003; McIntire et al., 2003). Kuchroo and colleagues independently identified Tim-3 as a Th1 cell-specific surface protein (Monney et al., 2002). Administration of anti-Tim-3 mAb or soluble Tim-3 proteins promoted the development of Th1-dependent immune responses including EAE (Monney et al., 2002; Sabatos et al., 2003; Sanchez-Fueyo et al., 2003). In this context, the Tim protein ligands, including Sema4A, are likely to be regulatory molecules influencing the activation and differentiation of T cells. However, it remains unknown how Sema4A is involved in regulating the differentiation of T cells into Th1 or Th2 effector cells.

Here, we generated and characterized Sema4A-deficient mice. These mice displayed several functional defects in the immune system, suggesting indispensable and essential roles for Sema4A. Sema4A-deficient DCs poorly stimulated allogeneic T cells. T cells from these mice also exhibited impaired in vitro Th1 differentiation. In Sema4A-deficient mice, both in vivo T cell primary and Th1 generation were impaired. Moreover, reconstitution experiments with antigen-pulsed DCs allowed us to identify the distinct roles for DC-derived and T cell-derived Sema4A in different phases of the immune responses.

Results

Generation of Sema4A-Deficient Mice

To evaluate the functions of Sema4A in vivo, we generated mice with a null mutation in the *Sema4A* locus. The targeting vector was constructed by replacing a 1.8 kb genomic region including the initiation codon with the neomycin (neo) resistance gene cassette to ensure disruption of Sema4A protein expression (Figure 1A). Transfection of ES cells with this construct resulted in two clones, each carrying one copy of the homologously recombined *Sema4A* mutant allele. Chimeric mice derived from one of these ES clones were found to transmit the mutant allele to their offspring. Homozygous mutant mice were produced in a typical Mendelian pattern and were viable (Figure 1B). Both female and male mutant mice appeared to develop normally and were fertile. RT-PCR analysis with total RNA from the spleen and cell surface staining of DCs confirmed the lack of Sema4A expression in homozygous mutants (Figures 1C and 1D). In macroscopic and histological examination, defects were not observed in the brain, kidney, lung, testis, and heart, in which Sema4A transcripts are expressed. We did not observe any differences in the cell surface phenotypes, numbers, and ratios of T cells and B cells in the spleen and thymus between Sema4A-deficient and wild-type mice (Figure S1; see the Supplemental Data available with this article online). However, as shown below, the mutant mice displayed functional defects in the immune system.

Involvement of Sema4A in T Cell Activation by DCs

We previously showed by using soluble Sema4A proteins and anti-Sema4A mAb that Sema4A expressed on the cell surface of DCs enhances T cell activation (Kumanogoh et al., 2002a). Therefore, we tested whether Sema4A contributes to an MLR by using MHC-mismatched T cells and DCs. DCs from Sema4A-deficient mice or wild-type littermates were used to stimulate allogeneic $CD4^+$ T cells. Sema4A-deficient DCs poorly stimulated allogeneic T cells compared to wild-type DCs (Figure 2A). In contrast, when $CD4^+$ T cells from Sema4A-deficient mice or wild-type littermates were cultured with allogeneic DCs from wild-type mice, no differences in the MLR were observed (Figure 2B), suggesting an important role for DC-expressed Sema4A in stimulating the MLR. Consistent with this observation, the levels of IL-2 in the culture supernatants were considerably reduced when Sema4A-deficient DCs were used as antigen presenting cells (APCs) in the MLRs (Table S1). However, Sema4A-deficient DCs produced IL-12 (Figure 2C) and upregulated MHC class II and costimulatory molecules (Figure 2D) to the same extent as wild-type DCs following anti-CD40 treatment. Collectively, these findings indicate that DC-derived Sema4A is directly and critically involved in the activation of T cells reactive to allo-antigens on DCs.

We next examined in vitro responses of Sema4A-deficient B cells to various stimuli. As shown in Figure 2E, the proliferative responses of Sema4A-deficient B cells to anti-CD40, LPS, or anti-μ were comparable to those of wild-type cells. Thus, the responses of B cells were not affected by the absence of Sema4A. We then examined the in vitro responses of Sema4A-deficient T cells. $CD62L^{high}$ $CD4^+$ naïve T cells were purified by cell sorting and were cultured with immobilized anti-CD3. T cells from Sema4A-deficient mice exhibited slightly but reproducibly reduced responses compared to T cells of wild-type mice (Figure 2F).

Preferential Expression of Sema4A during Th1 Differentiation

Although the expression of Sema4A is induced on activated T cells, the precise expression profiles and roles of Sema4A during activation and differentiation of T cells have not been determined. A slight reduction of anti-CD3-induced T cell proliferation led us to analyze the kinetics of Sema4A expression during in vitro T cell activation and differentiation. For this purpose, we generated a

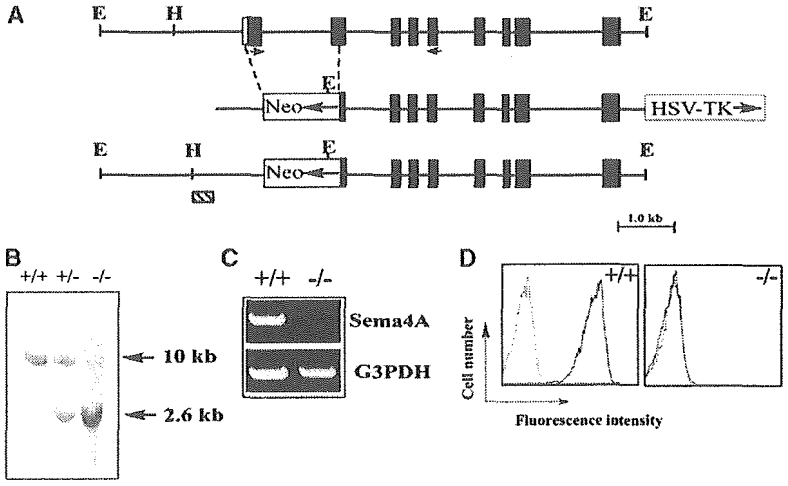

Figure 1. Generation of Sema4A-Deficient Mice

(A) Disruption of the *Sema4A* gene. The gene structure of the wild-type *Sema4A* allele (top), the Sema4A targeting construct (middle), and the resultant *Sema4A* mutant allele (bottom) are shown. Sema4A 5′ noncoding sequences are shown as open boxes, and coding sequences are shown as closed boxes. The 1.8 kb fragment containing the initiation codon was replaced with the neomycin resistance gene (Neo). The *HSV-tk* gene was appended to allow for selection against random integration. Arrows in the Neo cassettes indicate the transcriptional directions.

(B) Southern blot analysis. To assess the genotype of wild-type (+/+), heterozygous (+/–), and homozygous (–/–) mutant mice, tail DNAs were digested with EcoRI, electrophoresed, and hybridized with the probe that is shown by a hatched box in (A). The 10 kb fragment represents the wild-type *Sema4A* allele, and the 2.6 kb fragment depicts the targeted allele.

(C) RT-PCR analysis with RNAs of the spleen from wild-type (+/+) or Sema4A-deficient (–/–) mice. PCR was performed by using the indicated primers in (A) for Sema4A or G3PDH.

(D) Bone marrow-derived DCs from wild-type (+/+) or Sema4A-deficient (–/–) mice were stained with FITC-conjugated anti-CD11c, PE-conjugated anti-B220 and biotinylated anti-Sema4A mAb (solid lines) or isotype-matched controls (dotted lines) plus APC-conjugated streptavidin. The cells positive for CD11c and negative for B220 were gated and analyzed for Sema4A expression by flow cytometry.

high-affinity Sema4A mAb by immunizing Sema4A-deficient mice with Sema4A-Fc protein. This Sema4A mAb could detect the faint Sema4A expression on CD62L^{high} CD4^{+} naïve T cells, which we had failed to see when using a rat anti-Sema4A mAb in the previous study. Sema4A expression was maximally upregulated on T cells 24 hr after culture with anti-CD3 and anti-CD28, and its intensity gradually became weaker (Figure 3A, upper). We then investigated the expression profiles of Sema4A during in vitro Th differentiation. Naïve T cells prepared from wild-type or Sema4A-deficient mice were cultured with immobilized anti-CD3 plus anti-CD28 mAbs in the presence of IL-12 plus anti-IL-4 (Th1-skewing conditions) or in the presence of IL-4 plus anti-IL-12 and anti-IFN-γ (Th2-skewing conditions). Under the Th2-skewing conditions, Sema4A expression was transiently upregulated on T cells by 24 hr, and then its intensity became weaker (Figure 3A, lower), which is essentially identical to the kinetics of Sema4A expression on T cells stimulated with anti-CD3 and anti-CD28 (Figure 3A, upper). Notably, when T cells were cultured under Th1-skewing conditions, the intensity of Sema4A expression continued to increase (Figure 3A, middle). Furthermore, significantly upregulated Sema4A expression was persistently observed on Th1-polarized cells after three rounds of consecutive cultures under Th1-skewing conditions, while the intensity of Sema4A expression on Th2-polarized cells was almost comparable to that on resting T cells (Figure 3B). On the other hand, expression of Tim-2 was not detectable on the surface of resting T cells, but it was detected on T cells by 48 hr after stimulation (Figure S2). Cell surface expression of Tim-2 on Th1- or Th2-polarized cells was no longer detected. However, when restimulated, the expression of Tim-2 was induced on these cells as well (Figure S2).

Involvement of Sema4A in In Vitro Th1 Differentiation

The expression profiles of Sema4A suggest a role for T cell-derived Sema4A in Th differentiation. CD62L^{high} CD4^{+} naïve T cells prepared from wild-type or Sema4A-deficient mice were cultured for 5 days with immobilized anti-CD3 plus anti-CD28 mAbs in the presence of IL-12 plus anti-IL-4 (Th1-skewing conditions) or in the presence of IL-4 plus anti-IL-12 and anti-IFN-γ (Th2-skewing conditions). The numbers of Sema4A-deficient T cells recovered after 5 days of Th1-skewing culture were considerably lower compared to those of wild-type T cells by 35% ± 5%. We then restimulated the resulting Th1- or Th2-conditioned cells with anti-CD3 and measured the levels of IFN-γ and IL-4 in the culture supernatants. The production of IFN-γ by Th1-conditioned cells from Sema4A-deficient mice was severely impaired (Figure 4A, left), while the production of IL-4 was not detected in either Sema4A-deficient or wild-type Th1-condtioned cells (data not shown). In contrast, the production of IL-4 by Th2-conditioned cells from Sema4A-deficient mice was only slightly affected (Figure 4A, right). The production of IFN-γ was not detected in either Sema4A-deficient or wild-type Th2-condtioned cells (data not shown). Intracellular cytokine staining revealed that the population of IFN-γ-producing cells in Sema4A-deficient T cells was considerably reduced compared to wild-type T cells (Figure 4B, upper). In contrast, differences were not seen in the populations of IL-4-producing cells between Sema4A-deficient and wild-type T cells (Figure 4B, lower).

Although Sema4A functions as a cell surface ligand (Kumanogoh et al., 2002a), it is possible that the impaired in vitro Th1 differentiation might be caused by an unknown, intrinsic function of Sema4A rather than its inability to interact with binding partner(s) in the knockout mice. To exclude this possibility, Sema4A-

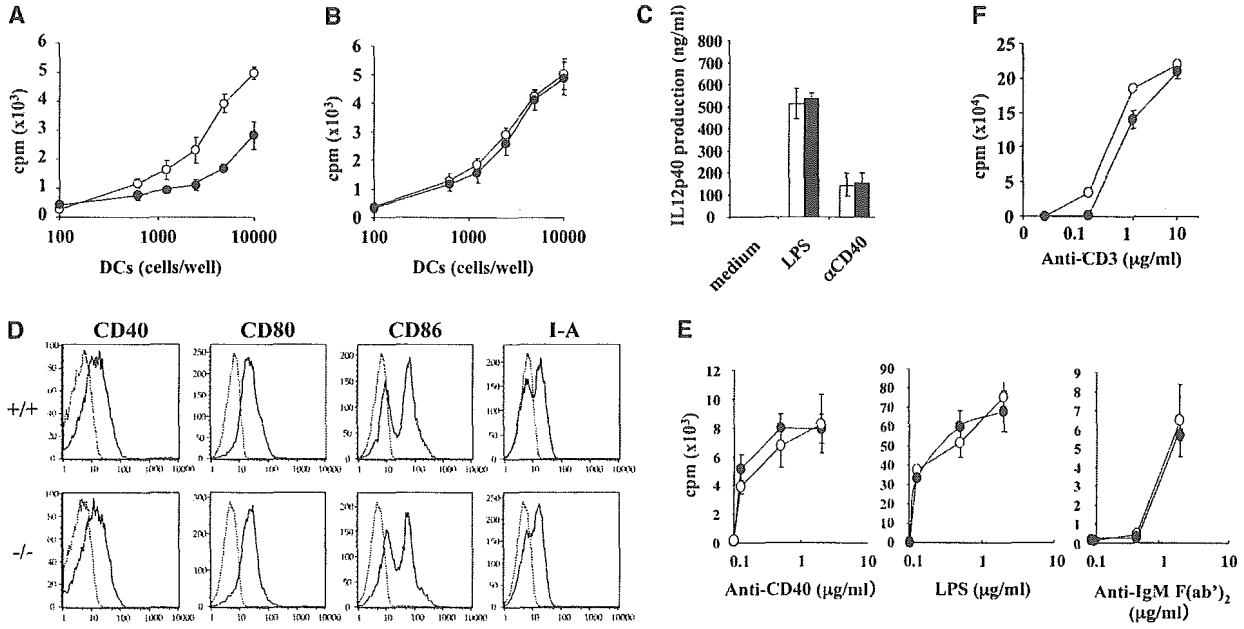

Figure 2. Reduced Allostimulatory Activities of DCs in Sema4A-Deficient Mice

(A) Reduced stimulatory activities against allogeneic T cells. Irradiated DCs derived from wild-type (open circles) or Sema4A-deficient DCs (closed circles) were cultured with allogeneic CD4+ T cells for 48 hr.

(B) Normal MLRs between wild-type and Sema4A-deficient CD4+ T cells. Irradiated DCs derived from wild-type mice were cultured with allogeneic wild-type (open circles) or Sema4A-deficient (closed circles) CD4+ T cells for 48 hr.

(C) Normal IL-12 production in Sema4A-deficient mice. Bone marrow-derived DCs from wild-type (white bars) or Sema4A-deficient DCs (black bars) were cultured for 72 hr with or without anti-CD40 or LPS.

(D) Normal expression of costimulatory molecules in Sema4A-deficient DCs. Bone marrow-derived DCs from wild-type (upper) or Sema4A-deficient DCs (lower) were cultured for 24 hr with anti-CD40 mAb. Cells were stained with PE anti-B220; FITC anti-CD11c; and biotin anti-CD40, anti-CD80, anti-CD86, or anti-I-A plus streptavidin APC. CD11c-positive and B220-negative cells were analyzed for the expression of CD40, CD80, CD86, and I-A.

(E) Normal B cell proliferative responses in Sema4A-deficient mice. Small resting B cells prepared from wild-type (open circles) or Sema4A-deficient mice (closed circles) were cultured for 72 hr with or without various concentrations of the indicated factors.

(F) Proliferative responses of naïve Sema4A-deficient T cells. CD62L^{high} CD4+ naïve T cells from wild-type (open circles) and Sema4A-deficient mice (closed circles) were purified by using FACS sorting and were cultured with various concentrations of immobilized anti-CD3 plus anti-CD28 for 48 hr. [^{3}H]-thymidine was added for the last 14 hr.

Error bars indicate mean ± SD.

deficient CD4+ naïve T cells (Ly5.2+) were cocultured with congenic wild-type CD4+ naïve T cells (Ly5.1+) under Th1-skewing conditions. The resulting Ly5.1-positive or -negative cells were gated, and INF-γ-producing cells were analyzed by intracellular cytokine staining (Figure 4C). The reduction in INF-γ-producing cells in Sema4A-deficient T cells was restored by coculture with wild-type T cells. Correspondingly, Ly5.1-negative cells derived from Sema4A-deficient mice produced comparable levels of IFN-γ after coculture with wild-type T cells (Figure S3), thus excluding possible influence of the intrinsic defects of Sema4A on in vitro Th1 differentiation.

Differentiation of T cells into Th1 or Th2 cells crucially

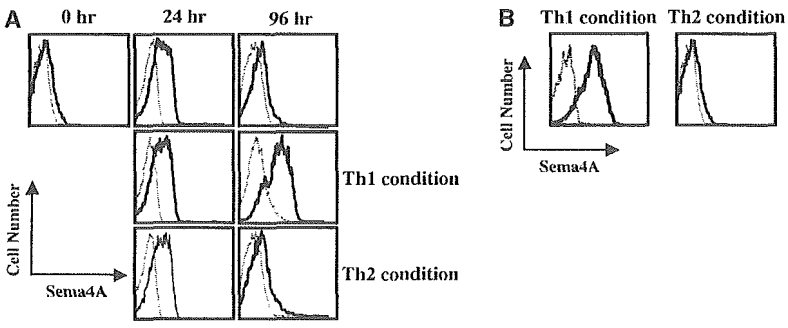

Figure 3. Preferential Expression of Sema4A during In Vitro Th1 Differentiation

(A) Expression profiles of Sema4A during T cell activation and differentiation. Naïve T cells were cultured with immobilized anti-CD3 and anti-CD28 in nonpolarizing, Th1-, or Th2-skewing conditions and then stained with biotinylated anti-Sema4A mAb (solid lines) or isotype-matched controls (dotted lines) plus streptavidin-conjugated APC and were analyzed by flow cytometry.

(B) Specific expression of Sema4A on Th1-polarized cells. CD62L^{high} CD4+ naïve T cells prepared from wild-type mice were cultured with immobilized anti-CD3 and anti-CD28 in Th1- or Th2-skewing conditions. The resulting cells after 3 weeks of culture in Th1- or Th2-skewing conditions were stained with biotinylated anti-Sema4A mAb (solid lines) or isotype-matched controls (dotted lines) plus streptavidin-conjugated APC and were analyzed by flow cytometry.

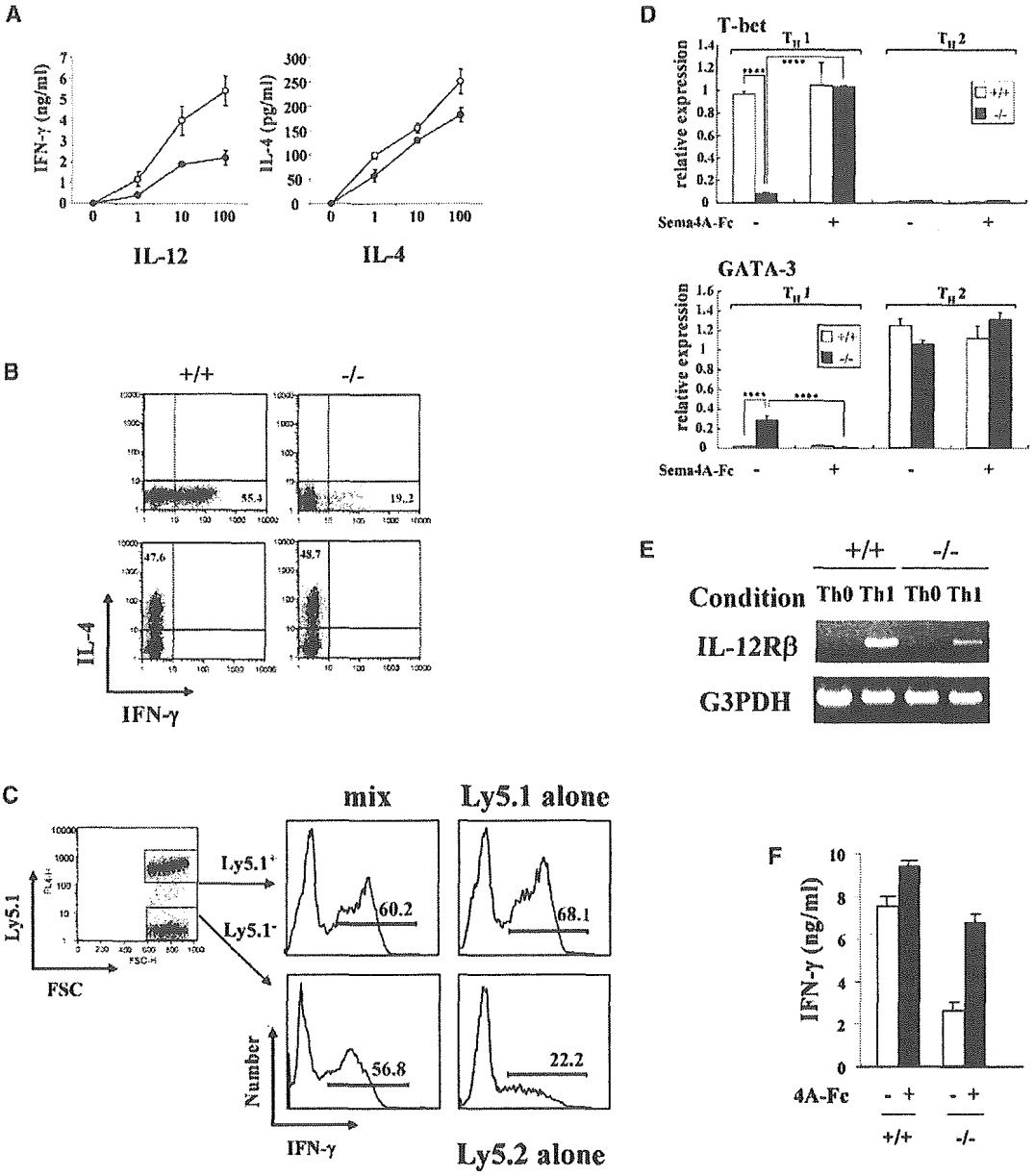

Figure 4. Involvement of Sema4A in In Vitro Th1 Differentiation

(A) Impaired in vitro differentiation of Sema4A-deficient T cells into Th1 cells. CD62L^{high} CD4^{+} naïve T cells prepared from wild-type (open circles) or Sema4A-deficient (closed circles) mice were cultured with immobilized anti-CD3 (2 μg/ml) and anti-CD28 (10 μg/ml) in Th1-skewing or Th2-skewing conditions. The resulting cells were restimulated with immobilized anti-CD3, and the levels of cytokines in the culture supernatants were measured by ELISA.

(B) Reduced IFN-γ-producing cell populations in Sema4A-deficient mice. CD62L^{high} CD4^{+} naïve T cells prepared from wild-type (left panels) or Sema4A-deficient (right panels) mice were cultured in Th1-skewing (upper panels) or Th2-skewing (lower panels) conditions for 5 days. The resulting cells were analyzed for intracellular cytokine staining.

(C) Restored in vitro Th1 differentiation of Sema4A-deficient T cells by coculture with wild-type T cells. Sema4A-deficient CD4^{+} naïve T cells (Ly5.2^{+}) were cocultured with congenic wild-type CD4^{+} naïve T cells (Ly5.1^{+}) under Th1-skewing conditions for 7 days. The resulting cells positive for Ly5.2^{+} or Ly5.1^{+} cells were gated for analysis of INF-γ-producing cells by intracellular cytokine staining.

(D) Reduced expression of T-bet in Th1-conditioned cells of Sema4A-deificient T cells. Naïve T cells prepared from wild-type (white bars) or Sema4A-deficient mice (black bars) were cultured in Th1- or Th2-skewing conditions with or without Sema4A-Fc. RNAs were prepared from day 4 Th1- or Th2-conditioned cells. Relative expression of T-bet and GATA-3 was determined by quantitative real-time PCR with the ribosomal RNA expression as the normalization controls. ****, $p < 0.001$. Each value was analyzed by using a paired t test.

(E) Reduced expression of IL-12Rβ2 in Sema4A-deficient T cells. Wild-type or Sema4A-deficient CD62L^{high} CD4^{+} naïve T cells purified by FACS sorting were cultured under Th0- or Th1-skewing conditions for 7 days. Expression of IL-12Rβ2 was determined by RT-PCR.

(F) Restored Th1 polarization of Sema4A-deficient T cells by Sema4A-Fc. CD62L^{high} CD4^{+} naive T cells prepared from wild-type or Sema4A-deficient mice were cultured under Th1-skewing conditions in the presence of Sema4A-Fc or control Fc proteins. The resulting cells were restimulated with immobilized anti-CD3, and the levels of IFN-γ in the culture supernatants were measured by ELISA.

Error bars indicate mean ± SD.